On the Sensitivity of the Equivalent Dynamic Stiffness Mapping Technique to Measurement Noise and Modelling Error

Javad Taghipour[a,*], Hamed Haddad Khodaparast[a], Michael I. Friswell[a], Hassan Jalali[b], Hadi Madinei[a], Nidhal Jamia[a]

[a] College of Engineering, Swansea University, Bay Campus, Fabian Way, Crymlyn Burrows, Swansea, SA1 8EN, United Kingdom

[b] Department of Mechanical Engineering, Arak University of Technology, Arak 38181-41167, Iran

Abstract

The objective of this study is to investigate the sensitivity of the Equivalent Dynamic Stiffness Mapping (EDSM) identification method to typical types of inaccuracy that are often present during the identification process. These sources of inaccuracy may include the presence of noise in the simulated/measured data, expansion error in the estimation of unmeasured coordinates, modelling error in the updated underlying linear model, and the error due to neglecting the higher harmonics in the nonlinear response of the system. An analytical study is performed to identify the structural nonlinearities of two nonlinear systems, a discrete three-DOF Duffing system and a cantilever beam with a nonlinear restoring force applied to the tip of the beam, considering the presence of all the aforementioned sources of inaccuracy. First, the EDSM technique is utilized to identify the nonlinear elements of two example systems to verify the accuracy of the EDSM technique. Finite Element modelling, the Modified Complex Averaging Technique (MCXA), and arc-length continuation are exploited in this study to obtain the steady state dynamics of the nonlinear systems. Numerical models of the two systems are then simulated in MATLAB and the numerical results of the simulation are used to identify the unknown nonlinear elements using the EDSM technique and investigate the effect of different sources of error on the outcome of the identification process. The nonlinear response of the system has been regenerated using the identified parameters with the sources of error present and the generated response has been compared to the simulated response in the absence of any noise or error. The EDSM technique is capable of identifying accurately the nonlinear elements in the absence of any source of inaccuracy although, based on the results, this method is highly sensitive to the aforementioned sources of inaccuracy that results in significant error in the identified model of the nonlinear system. Finally, an optimization-based framework, developed by the authors, is utilized to identify the nonlinear cantilever beam and the results are compared with the results of the EDSM technique. It is shown that by using the optimization method, the inaccuracy due to different sources of noise and error is significantly reduced. Indeed, by using the optimization method, the necessity to use an expansion method and consider the higher harmonics of the response is eliminated.

Key words: Nonlinear structural dynamics, Identification, Model updating, Equivalent Dynamic Stiffness Mapping, Sensitivity to noise and error.

1 Introduction

Nonlinear behaviour is very likely to occur in most practical structures due to the effects of material properties, structural joints and boundary conditions. However, in many applications, the nonlinearity is small enough so that the structure is analysed using linear theories. On the other hand, there are unknown strong nonlinearities in many structures making it difficult to predict accurately the dynamic behaviour of the structures using linear analysis. Therefore, an appropriate nonlinear model is required to investigate the dynamics of the system. As a consequence, identification (localization, characterization and quantification) of such nonlinearities has received significant attention over recent decades.

There are many well-developed model updating and linear modal analysis methods for linear structures [1-4]. However, many of these methods are not directly applicable to nonlinear systems. There has been a wide range of studies in the literature focusing on identification and characterization of the nonlinear elements. One may find comprehensive reviews of system identification approaches in [5-9]. The following paragraphs provide a brief literature review of system identification methods for nonlinear dynamical structures.

The literature has an extensive range of identification approaches such as the force-state mapping technique, the restoring force surface method, the Hilbert transform, Bayesian system identification, Volterra series approximation, optimization-based identification approach, and the Equivalent Dynamic Stiffness Mapping technique [10-23]. Some methods assume the type of the nonlinearity is pre-known, and others do not rely on this assumption. Kerschen et al. [14] investigated the performance of the restoring force surface method in identifying nonlinear structural elements. In this regard, they considered the vibrations of a clamped beam with two different types of nonlinearities. Their method requires the displacement, velocity, acceleration and force of all degrees of freedom to be measured in the time domain. Feldman [15] recommended a nonparametric technique for identification of nonlinear elastic force functions based on the Hilbert transform. The method presented by Feldman does not require a priori information about the system structure or its parameters.

Worden and Hensman [17] surveyed the benefits and limitations of using the Bayesian approach for identification of nonlinear structural systems. This approach is not limited to any assumption regarding the type and parameters of the system nonlinearity. Using a combination of time and frequency domain techniques, Haroon et al. [21] presented a method to identify nonlinear systems in the absence of input measurements. Taghipour et al. [22] proposed an optimization-based identification approach in order to avoid different sources of error in the identification process. According to this framework, it is not necessary to have complete measurement of the response at all coordinates. Therefore, using expansion methods (e.g. SEREP) is not required in the case of incomplete measurements. The Equivalent Dynamic Stiffness Mapping technique was proposed by Wang and Zheng [23] for identification of nonlinear structural elements in dynamical systems using steady-state primary harmonic frequency response functions (FRF). There is no need for the type and parameters of the nonlinearity to be pre-known in this method, however having knowledge of the type of nonlinear element leads to a better parameter estimation and identification of the system.

Unlike the numerical simulation of theoretical problems, the experimental study of practical structures is never free of noise. As the model of underlying linear system is an essential

requirement in the identification of nonlinear systems and investigation of their dynamics, having an accurate linear model of the underlying linear system is very important. On the other hand, the presence of nonlinearity in the system yields modelling errors in the updating of the linear model. Furthermore, the complexity of the structure, insufficient sensors, and the high cost of experiments, often make it impossible to have complete measurements at all coordinates of the nonlinear system. Therefore, due to the existence of noise and modelling errors, an additional error may occur in the estimation of the responses at the unmeasured coordinates.

The response of nonlinear systems is usually a multi-harmonic (including sub- or super-harmonics) behaviour. In many problems, the sub- or super-harmonics of the response are significant and cannot be neglected. Therefore, considering only primary harmonic of the response may be errorsome. The aforementioned noise and errors may lead to errors in the results of the identification methods. This study is focused on the investigation of the sensitivity of the Equivalent Dynamic Stiffness Mapping technique (EDSM) [23] to experimental noise and various types of errors and showing the advantages of an optimisation based approach in the presence of measurement noise.

In this paper, both theoretical and experimental studies are carried out to analyse the sensitivity of the EDSM technique to noise and error. In this regard, the accuracy of the application of the EDSM technique is verified using numerical simulation of a nonlinear discrete multi-degree-of-freedom (MDOF) system and a nonlinear cantilever beam. Steady state responses of numerical simulations are obtained by utilizing the Modified Complex Averaging (MCXA) technique [24, 25] and numerical arc-length continuation. Considering various types of noise and error, the sensitivity of the EDSM technique is studied using both theoretical results of both discrete and continuous nonlinear systems. It is concluded that contaminated data used for the identification may lead to errors in the results of the EDSM identification. Then, an optimization-based framework introduced by Taghipour et al. [22] is utilized to identify the nonlinear system of the cantilever beam. By using the optimization method, one may reduce the inaccuracy arising from the aforementioned sources of noise and errors. The nonlinear response of the system obtained from the optimization method and the EDSM technique are compared with the simulated response of the system. It is shown that by using the optimization method, the use of an expansion method and consideration of the higher harmonics of the response are not required. Finally, a brief conclusion of the study is presented.

2 Theory

The Equivalent Dynamic Stiffness Mapping Technique is explained in Section 2.1. In order to obtain the dynamical response of the system in the numerical simulation, the semi-analytic Modified Complex-Averaging (MCXA) method is used along with the numerical arc-length continuation method. The MCXA method is briefly described in Section 2.2.

2.1 Equivalent Dynamic Stiffness Mapping Technique

The governing equation of a general nonlinear dynamical system can be considered as,

$$[\mathbf{M}]\{\ddot{\boldsymbol{x}}(\boldsymbol{t})\} + [\mathbf{C}]\{\dot{\boldsymbol{x}}(\boldsymbol{t})\} + [\mathbf{K}]\{\boldsymbol{x}(\boldsymbol{t})\} + \{\boldsymbol{f_{nl}}(\boldsymbol{t})\} = \{\boldsymbol{f}(\boldsymbol{t})\} \quad (1)$$

where $[\mathbf{M}]$, $[\mathbf{C}]$ and $[\mathbf{K}]$ are mass, damping and stiffness matrices, respectively. $\{\boldsymbol{f}(\boldsymbol{t})\}$, $\{\boldsymbol{x}(\boldsymbol{t})\}$ and $\{\boldsymbol{f_{nl}}(\boldsymbol{t})\}$ are respectively the applied force, response and nonlinear restoring force vectors. Considering that the external applied force is harmonic, i.e. $\{\boldsymbol{f}(\boldsymbol{t})\} = \{\mathbf{F}_{ex}\}\boldsymbol{e^{j\omega t}}$, the response and nonlinear force vector can be considered harmonic too as $\{\boldsymbol{x}(\boldsymbol{t})\} = \{\mathbf{X}\}\boldsymbol{e^{j\omega t}}$ and $\{\boldsymbol{f_{nl}}(\boldsymbol{t})\} = \{\mathbf{F}_{NL}\}\boldsymbol{e^{j\omega t}}$. By substituting the assumed force and response vectors into equation (1) one obtains,

$$\mathbf{F}_{NL} = \mathbf{F}_{ex} - (\mathbf{K} + j\omega\mathbf{C} - \omega^2\mathbf{M})\mathbf{X}, \tag{2}$$

where $\mathbf{F}_{ex}$ and $\mathbf{X}$ are the vectors of the external force and the response of the system in the frequency domain and $j = \sqrt{-1}$. As the type of nonlinearity is unknown, it is assumed to be composed of both nonlinear stiffness and nonlinear damping as

$$\mathbf{F}_{NL} = \mathbf{D_{eq}}\mathbf{X} = \left(\mathbf{K}_{eq} + j\omega\mathbf{C}_{eq}\right)\mathbf{X}, \tag{3}$$

where $\mathbf{K}_{eq}$ and $\mathbf{C}_{eq}$ denote, respectively, the equivalent stiffness and damping elements of the nonlinear internal force. The unknown Equivalent Dynamic Stiffness $\mathbf{D_{eq}}$ of the internal force is defined as the ratio of the nonlinear internal force to the displacement response of the system in the frequency domain. However, as the total number of unknowns in $\mathbf{D_{eq}}$ is more than the number of equations in Eq. (3), it cannot be solved as a system of linear equations. Indeed, the elements of $\mathbf{D_{eq}}$ at which there is no nonlinear element should be zero. In addition, $\mathbf{D_{eq}}$ is a symmetric matrix. That is, in case of ungrounded (connected) nonlinearities between two DOFs i and j, $D_{eq_{ij}} = D_{eq_{ji}}$. Therefore, instead of solving Eq. (3) as a system of equations to find the matrix $\mathbf{D_{eq}}$, it is solved individually for each nonlinear element.

It is taken for granted that prior to the characterization of the nonlinear element, the exact location of the nonlinearity, i.e. whether it is grounded or ungrounded and the involved DOFs, has been determined. Accordingly, for grounded nonlinearities, in which only one degree of freedom is involved, the equivalent dynamics stiffness D_{ii}, is obtained as

$$D_{ii} = \frac{f_{N_i}}{X_i}, \tag{4}$$

The real and imaginary parts of the equivalent dynamics stiffness give the equivalent nonlinear stiffness $k_{eq_{ii}}$ and equivalent nonlinear damping $c_{eq_{ii}}$ of the nonlinear internal force,

$$k_{eq_{ii}} = \Re(D_{ii}), \;\; c_{eq_{ii}} = \frac{\Im(D_{ii})}{\omega}, \tag{5}$$

For the case of ungrounded (connected) nonlinearities the relations of Eqs. (4) and (5) become

$$D_{ij} = \frac{f_{N_i}}{X_i - X_j}, \;\; k_{eq_{ij}} = \Re\left(D_{ij}\right), \;\; c_{eq_{ij}} = \frac{\Im\left(D_{ij}\right)}{\omega}, \tag{6}$$

where D_{ij}, $k_{eq_{ij}}$, and $c_{eq_{ij}}$ are the element of dynamic stiffness, equivalent nonlinear stiffness, and equivalent nonlinear damping between DOF-i and DOF-j. Table 1 includes different types of internal forces and their ideal equivalent dynamic stiffness [23].

Table 1- Different types of internal forces and their ideal equivalent dynamic stiffness [23].

Type of internal force	Exact internal force	Ideal Equivalent Dynamic Stiffness
Linear spring	$f_{NL} = kx$	$D_{eq} = k$
Viscous damping	$f_{NL} = c\dot{x}$	$D_{eq} = j\omega c$
Cubic stiffness spring	$f_{NL} = kx^3$	$D_{eq} = \frac{3}{4}k\|X\|^2$

It is worth mentioning that the EDSM technique is based on some assumptions and has some limitations:

- As the identification procedure of the described method utilizes deterministic FRFs, the method requires steady state responses. Therefore, it should be ensured that the steady state response is measured and used in the calculations.
- All of the coordinates are required to be known. If some DOFs are not measured, they should be estimated utilizing an expansion method (e.g. SEREP) that may result in some inaccuracy.
- The method is based on the assumption that the primary harmonic is dominant and all other harmonics of the response are neglected.
- In practical systems, particularly in multi-DOF systems with strong nonlinearities and a flexible structure, there may be ill-conditioning problems in calculating the equivalent dynamic stiffness.

2.2 Semi-analytic Treatment and Numerical Simulation

For the theoretical analysis, the steady state dynamic response of the system subject to harmonic external force is obtained using the modified complex averaging technique (MCXA), [24, 25]. In order to use this technique, the response of the *i*-th degree of freedom $x_i(t)$ is approximated using the sum of the static response x_{st_i} and N_H harmonics of the dynamic response $x_i^n(t)$,

$$x_i(t) = x_{st_i} + \sum_{n=1}^{H} x_i^n(t)\,, \qquad i = 1, \dots, N_i, \tag{7}$$

where N_i is the number of degrees of freedom of the system. Defining new complex variables on each harmonic

$$\psi_i^n = \dot{x}_i^n + jn\omega x_i^n = \varphi_i^n e^{jn\omega t}, \qquad \bar{\psi}_i^n = \dot{x}_i^n - jn\omega x_i^n = \bar{\varphi}_i^n e^{-jn\omega t}, \tag{8}$$

where ω is the excitation frequency, the displacement $x_i^n(t)$ and derivatives $\dot{x}_i^n(t)$ and $\ddot{x}_i^n(t)$ can be derived for each harmonic of every degree of freedom as below.

$$\begin{gathered} x_i^n = \frac{1}{2jn\omega}\left(\varphi_i^n e^{jn\omega t} - \bar{\varphi}_i^n e^{-jn\omega t}\right), \dot{x}_i^n = \frac{1}{2}\left(\varphi_i^n e^{jn\omega t} + \bar{\varphi}_i^n e^{-jn\omega t}\right), \\ \ddot{x}_i^n = \frac{\left(\dot{\varphi}_i^n e^{jn\omega t} + \dot{\bar{\varphi}}_i^n e^{-jn\omega t}\right)}{2} + \frac{jn\omega}{2}\left(\varphi_i^n e^{jn\omega t} - \bar{\varphi}_i^n e^{-jn\omega t}\right) \end{gathered} \tag{9}$$

Substituting Eqs. (8) and (9) into the governing equation of the system and averaging over each harmonic, $N_i \times N_H$ new first order differential equations are obtained in terms of new complex variables φ_i^n. The complex variables φ_i^n are separated into real and imaginary parts.

$$\varphi_i^n = y_{2((i-1)N_H+n)-1} + jy_{2((i-1)N_H+n)} \ , \qquad i = 1, \dots, N_i, \tag{10}$$

Substituting Eq. (10) into the equation of motion of the system, $2 \times N_i \times N_H$ first order differential equations are derived in the general form as below

$$\dot{\mathbf{Y}} = \mathbf{R}(\mathbf{Y}), \tag{11}$$

where $\mathbf{Y} = \left[y_1 y_2 \dots y_{2\times N_i \times N_H}\right]^T$ is the unknown vector and $\dot{\mathbf{Y}} = \left[\dot{y}_1 \dot{y}_2 \dots \dot{y}_{2\times N_i \times N_H}\right]^T$ is the derivative of *Y*. For the case of steady state dynamics, eliminating the time derivatives $\dot{\mathbf{Y}} = \left[\dot{y}_1 \dot{y}_2 \dots \dot{y}_{2\times N_i \times N_H}\right]^T$ results in algebraic equations in the form

$$\mathbf{R}(\mathbf{Y}) = 0, \tag{12}$$

For nonlinear systems, it would be difficult or in many cases impossible to find an explicit analytic solution. Hence, in this study, pseudo arc-length continuation method has been used to solve the nonlinear Eqs. (12) and compute unknown variables $y_k, k = 1, \dots, 2 \times N_i \times N_H$, by which amplitude of each harmonic can be determined.

$$X_i^n = \frac{\sqrt{\left(y^2_{2((i-1)N_H+n)-1} + y^2_{2((i-1)N_H+n)}\right)}}{n\omega}, \tag{13}$$

Stability analysis of the steady state solution of the nonlinear system is also performed using Lyapunov's first method of stability analysis and simple linearization of Eq. (13) and considering the eigenvalues of the Jacobian matrix at equilibrium.

3 Verification

In this section, the accuracy of the semi-analytic MCXA technique and the EDSM method, respectively, in estimating the steady state response of nonlinear dynamic systems and identifying nonlinear systems is verified. For this purpose, the steady state dynamic response of two systems is considered. The first system is a 3DOF mass-spring system shown in Figure 1,

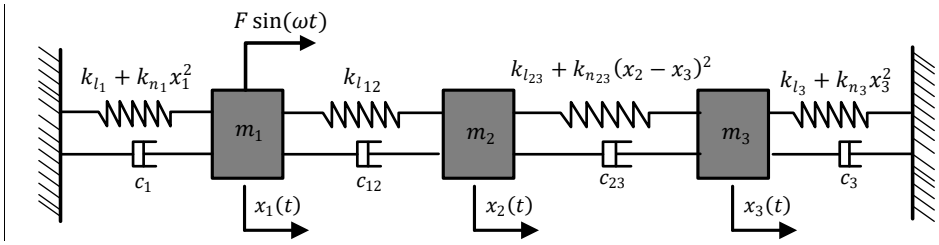

Figure 1- Three-DOF discrete nonlinear system.

The governing equations of the system is derived using Newton's second law as

$$\begin{aligned} m_1\ddot{x}_1 + c_1\dot{x}_1 + k_{l_1}x_1 + k_{n_1}{x_1}^3 + c_{12}(\dot{x}_1-\dot{x}_2) + k_{l_{12}}(x_1-x_2) &= F\sin(\omega t) \\ m_2\ddot{x}_2 + c_{12}(\dot{x}_2-\dot{x}_1) + k_{l_{12}}(x_2-x_1) + c_{23}(\dot{x}_2-\dot{x}_3) + k_{l_{23}}(x_2-x_3) & \\ + k_{n_{23}}(x_2-x_3)^3 = 0 & \\ m_3\ddot{x}_3 + c_3\dot{x}_3 + k_{l_3}x_3 + k_{n_3}{x_3}^3 + c_{23}(\dot{x}_3-\dot{x}_2) + k_{l_{23}}(x_3-x_2) + k_{n_{23}}(x_3-x_2)^3 &= 0, \end{aligned} \tag{14}$$

where m_1, m_2 and m_3 are the masses of the oscillators, c_1, c_{12}, c_{23}, c_3 are damping coefficients, $k_{l_1}, k_{l_{12}}, k_{l_{23}}, k_{l_3}$ are linear stiffnesses and $k_{n_1}, k_{n_{23}}, k_{n_3}$ denote the coefficients of nonlinear cubic stiffness. A harmonic external force with an amplitude of F and excitation frequency of ω is applied to the first degree of freedom. Table 2 contains the values given to the parameters of the system of Eq. (14) used for numerical simulations in this study.

Table 2- Values for the parameters of the system shown in Figure 1.

Parameters (unit)	**value**	**Parameters (unit)**	**value**	**Parameters (unit)**	**value**
$\boldsymbol{m_1}$ **(kg)**	1	$c_{23}\left(\frac{\text{N.s}}{\text{m}}\right)$	0.25	$k_{l_{23}}\left(\frac{\text{N}}{\text{m}}\right)$	30
$\boldsymbol{m_2}$ **(kg)**	2	$c_3\left(\frac{\text{N.s}}{\text{m}}\right)$	0.15	$k_{n_{23}}\left(\frac{\text{N}}{\text{m}^3}\right)$	300
$\boldsymbol{m_3}$ **(kg)**	1.5	$k_{l_1}\left(\frac{\text{N}}{\text{m}}\right)$	25	$k_{l_3}\left(\frac{\text{N}}{\text{m}}\right)$	30
$\boldsymbol{c_1}\left(\frac{\text{N.s}}{\text{m}}\right)$	0.1	$k_{n_1}\left(\frac{\text{N}}{\text{m}^3}\right)$	400	$k_{n_3}\left(\frac{\text{N}}{\text{m}^3}\right)$	500
$\boldsymbol{c_{12}}\left(\frac{\text{N.s}}{\text{m}}\right)$	0.2	$k_{l_{12}}\left(\frac{\text{N}}{\text{m}}\right)$	50	F (N)	1.5

It is assumed that all parameters are known except c_1, c_3, k_{l_1}, k_{n_1}, $k_{n_{23}}$, k_{l_3}, k_{n_3}. Accordingly, the mass, damping and stiffness matrices and the vector of nonlinear forces for the system shown in Figure 1 is defined as,

$$M=\begin{bmatrix} m_1 & 0 & 0 \\ 0 & m_2 & 0 \\ 0 & 0 & m_3 \end{bmatrix},\qquad C=\begin{bmatrix} c_{12} & -c_{12} & 0 \\ -c_{12} & c_{12}+c_{23} & -c_{23} \\ 0 & -c_{23} & c_{23} \end{bmatrix},$$
$$K=\begin{bmatrix} k_{l_{12}} & -k_{l_{12}} & 0 \\ -k_{l_{12}} & k_{l_{12}}+k_{l_{23}} & -k_{l_{23}} \\ 0 & -k_{l_{23}} & k_{l_{23}} \end{bmatrix},$$
$$\{f_{NL}\}=\begin{Bmatrix} c_1\dot{x}_1+k_{l_1}x_1+k_{n_1}{x_1}^3 \\ k_{n_{23}}(x_2-x_3)^3 \\ c_3\dot{x}_3+k_{l_3}x_3+k_{n_3}x_3^3+k_{n_{23}}(x_3-x_2)^3 \end{Bmatrix}, \tag{15}$$
$$\{f(t)\}=\begin{Bmatrix} F\sin(\omega t) \\ 0 \\ 0 \end{Bmatrix},$$

Therefore, Eq. (14) is rearranged in matrix form so that the vector of nonlinear force $\{f_{NL}\}$ includes only unknown parameters, which are identified using the Equivalent Dynamic Stiffness Mapping technique.

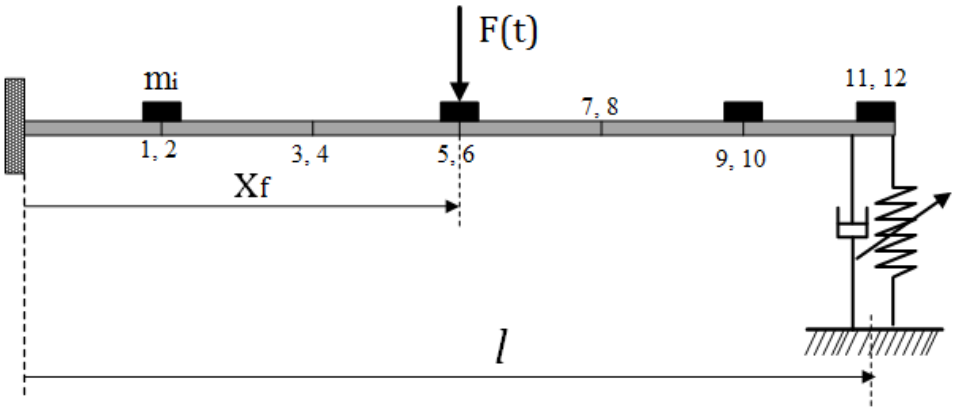

Figure 2- Schematic of the cantilever beam with a grounded nonlinear restoring force at the tip.

A nonlinear stainless-steel cantilever beam subject to an external harmonic force is considered as the second system studied in this paper. The beam is assumed to have the geometry and material properties given in Table 3. As shown in Figure 2, a nonlinear restoring force is applied to the tip of the beam through a grounded nonlinear attachment including a nonlinear spring (a linear and a cubic stiffness) and a linear dashpot. The nonlinear restoring force and parameters are given as

$$f_{NL}=c_l\dot{w}(l,t)+k_l w(l,t)+k_N w(l,t)^3, \tag{16}$$

where

$$c_l=0.004\frac{\mathrm{N.s}}{\mathrm{m}},\qquad k_l=20\frac{\mathrm{N}}{\mathrm{m}},\qquad k_N=1\times10^5\frac{\mathrm{N}}{\mathrm{m}^3}. \tag{17}$$

and $w(l,t)$ denotes the deflection of the beam at the tip. Harmonic point force $F_{ex}(t)=f\sin(\omega t)$ excitation is used to excite the beam. In the configuration of the beam in Figure 2, there are four point masses $p_m=\{6,6,6,8\}$ g respectively located at positions $x_m=\left\{\frac{l}{6},\frac{3l}{6},\frac{5l}{6},l\right\}$ from the

clamped end of the beam, where l is the beam length. Tip mass represents the mass of bolts and nuts used to attach spring and dashpot to the beam. The three other masses represent the mass of accelerometers used to measure the response of the beam.

Table 3- Geometry and material properties of the beam shown in Fig. 2.

Length	$\mathbf{0.30\ m}$
Width	30 mm
Thickness	1.5 mm
Modulus of Elasticity, E	205 GPa
Density, ρ	$7800\frac{\text{kg}}{\text{m}^3}$
Damping coefficient per length, γ	$0.2\frac{\text{kg}}{\text{m.s}}$

According to Euler-Bernoulli beam theory [26] and utilizing the Finite Element method and six two-node linear Euler-Bernoulli beam elements, the given nonlinear structure is governed by following equation in matrix form

$$\mathbf{M}\ddot{\mathbf{w}}(t) + \mathbf{C}\dot{\mathbf{w}}(t) + \mathbf{K}\mathbf{w}(t) + \boldsymbol{f}_{NL}(\mathbf{w}, \dot{\mathbf{w}}) = \boldsymbol{f}_{ex}(t), \tag{18}$$

where $\mathbf{M}, \mathbf{K}, \mathbf{C}$ denote the global mass, stiffness, and damping matrices, respectively. $\mathbf{w}(t)$ is the time response of the beam at instant time t. The vectors of displacement and its time derivatives are shown by $\mathbf{w}(t)$, $\dot{\mathbf{w}}(t)$, and $\ddot{\mathbf{w}}(t)$, respectively. $\boldsymbol{f}_{nl}(\mathbf{w}, \dot{\mathbf{w}})$ is the unknown nonlinear internal force of the system.

3.1 Verification of the MCXA Technique

In order to verify the accuracy of the MCXA method, the 3DOF system of Figure 1 is considered. The steady state dynamics of the system of Eq. (14) with parameters of Table 2 is obtained using the MCXA technique and ODE direct integration in MATLAB. Then, the results of the two methods are compared.

To simulate the response of the system using MCXA, the first three harmonics of the response are considered. Figures 3 and 4 illustrates the amplitude-frequency and phase-frequency diagrams of the first three harmonics of the steady state dynamics of the system. $|X_{H_i}|$ and φ_{H_i} in Figures 3 and 4 denote, respectively, the amplitude and phase of i-th harmonic of the steady state response. Stable and unstable branches of the steady state response are shown by blue and red lines, respectively. The stability of the steady state response of the system was investigated using Lyapunov's first method of stability analysis.

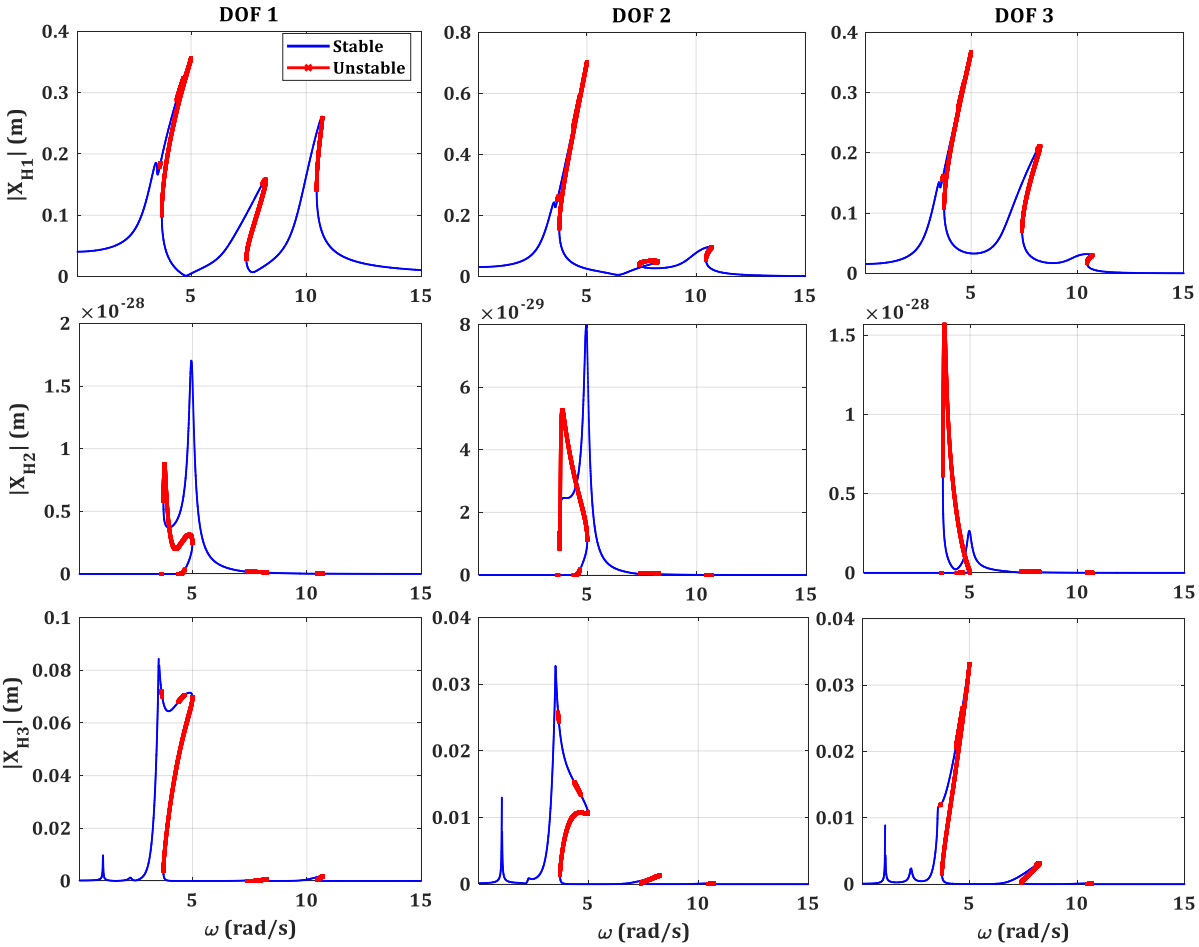

Figure 3- Amplitude–frequency diagram of the first three harmonics of the steady state response of the 3DOF system. Blue lines denote the stable branches and red lines represent the unstable branches.

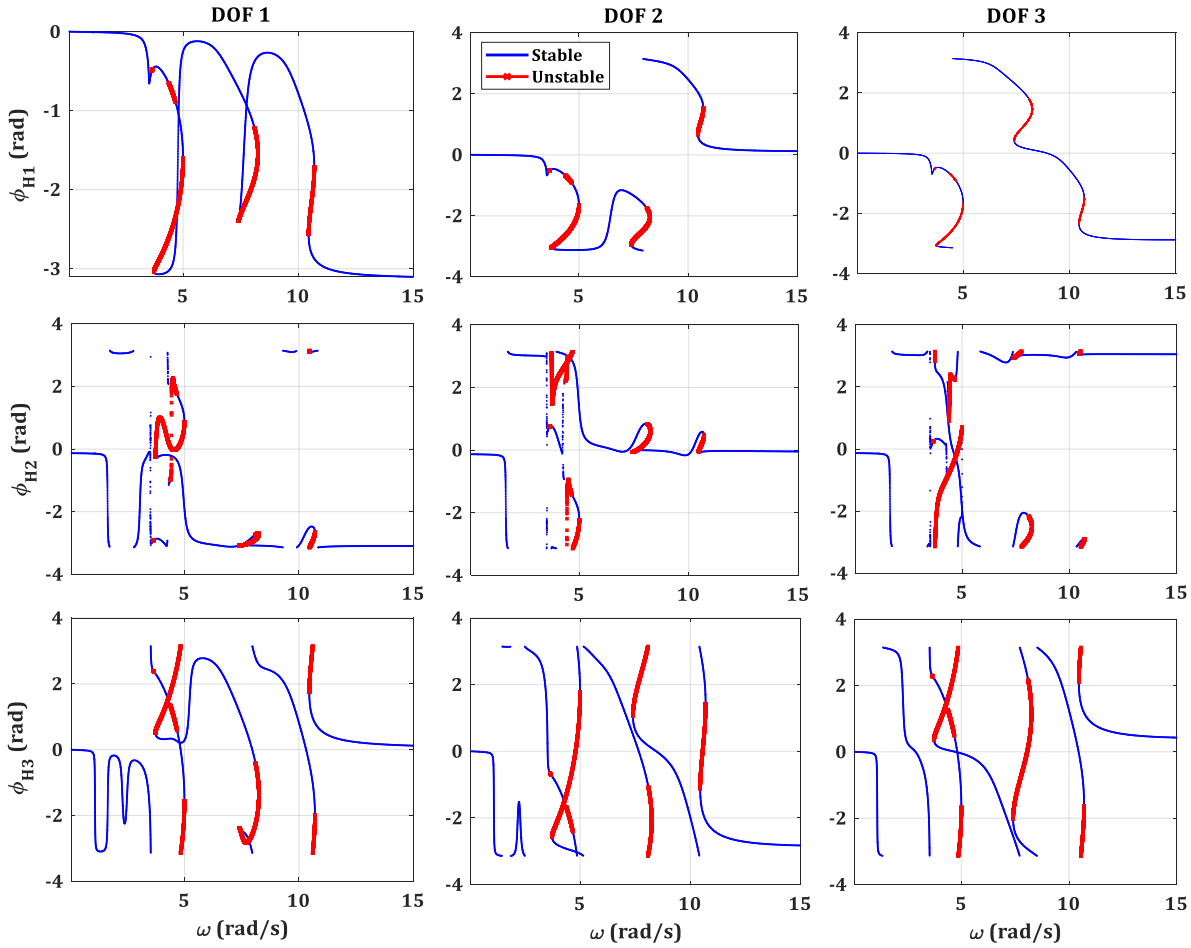

Figure 4- Phase–frequency diagram of the first three harmonics of the steady state response of the 3DOF system. Blue lines denote the stable branches and red lines represent the unstable branches.

Figure 5 illustrates the comparison between the first and third harmonics of the steady state dynamics of the 3DOF system obtained using the MCXA technique and ODE integration in MATLAB. As expected, ODE integration is not capable of estimating the unstable solutions. ODE integration cannot even predict some of the stable solutions due to the limited stability range at some points. However, there is a good compatibility between the results obtained by the MCXA technique and the results estimated using ODE integration.

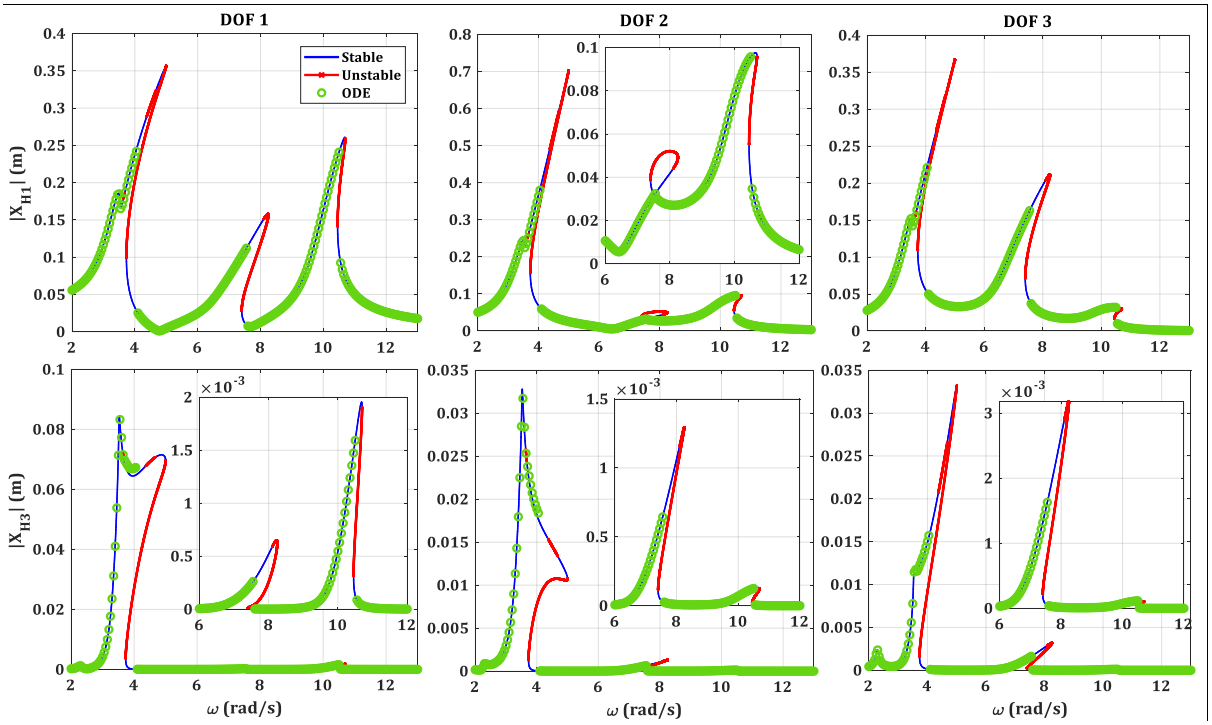

Figure 5- Comparison between the first and third harmonics of the steady state response of the 3DOF system obtained by the MCXA technique and ODE integration.

Figure 6 shows the comparison between the time history of the steady state response of the 3DOF system at $\omega = 3.5$ rad/s obtained using the MCXA technique and ODE integration. Figure 6(a) illustrates the multi-harmonic response of the system, while Figures 6(b) and 6(c) demonstrate, respectively, the first and third harmonics of the response. The results show a good compliance between the two different methods. However, since the MCXA technique is able to obtain both stable and unstable branches of the response, and also has a much lower computational cost than ODE integration, the MCXA technique is used here in this study.

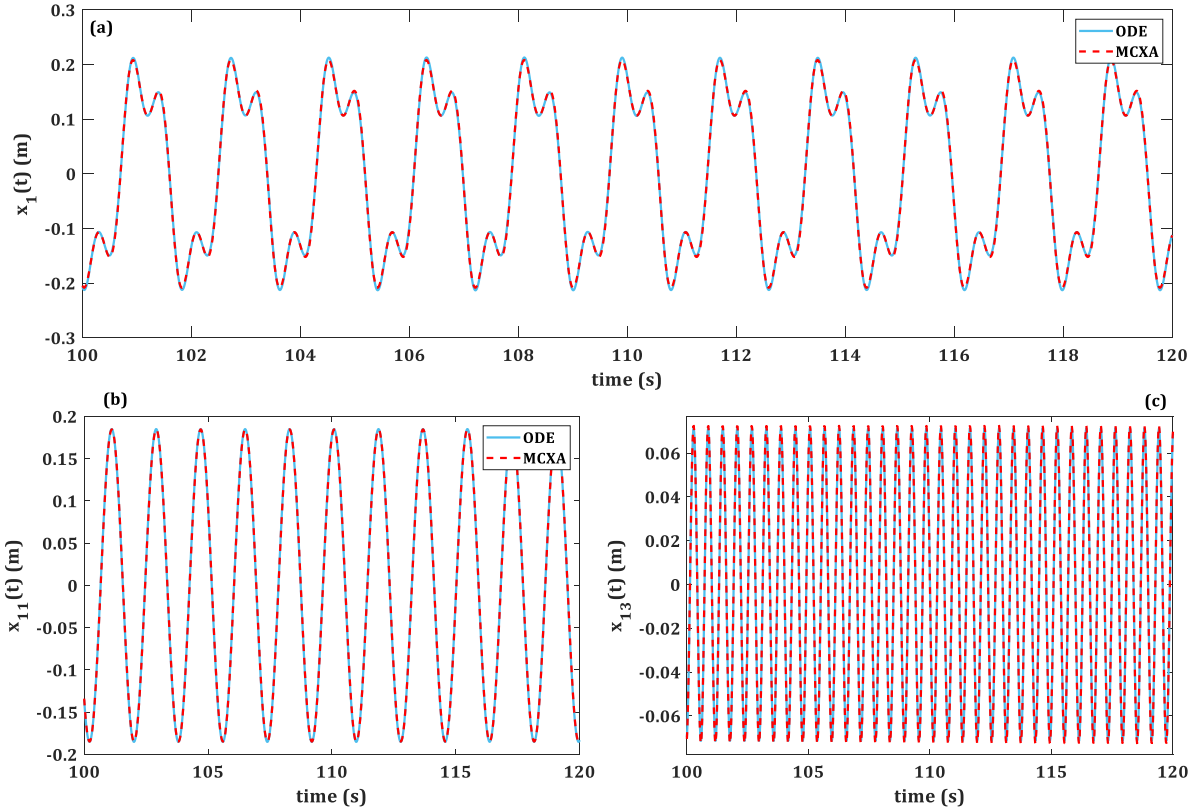

Figure 6- Comparison between the time history of the first degree of freedom of the 3DOF system obtained using MCXA and ODE integration. (a) Multi-harmonic response; (b) primary harmonic; (c) third harmonic.

3.2 Verification of the EDSM Technique

In this section, the accuracy of the EDSM method is verified in the absence of any noise and error. For this purpose, the steady state dynamics of the two example nonlinear systems are obtained using the MCXA technique and arc-length continuation. The nonlinear forces of the two systems are identified using the EDSM technique.

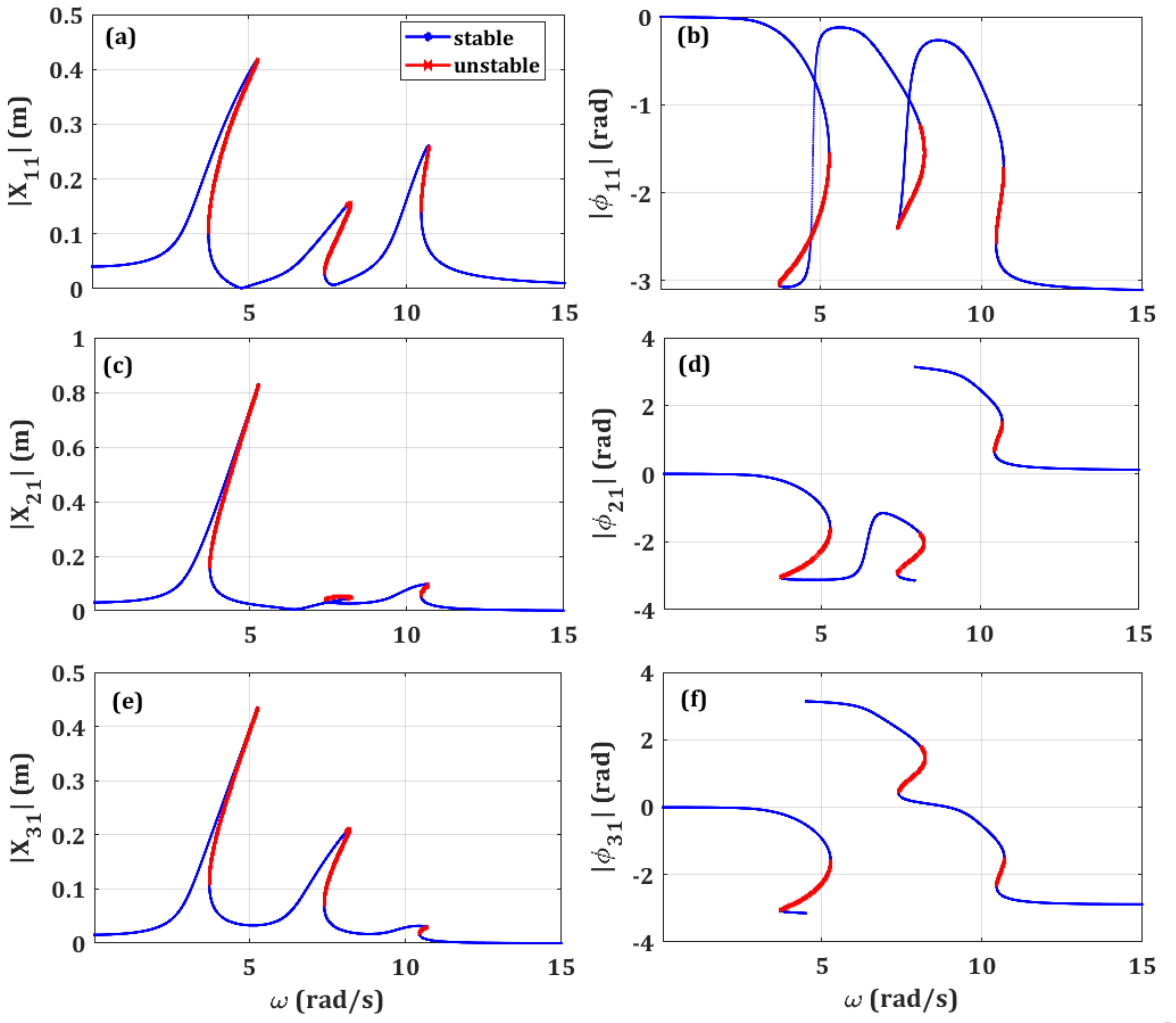

Figure 7- (a, c, e) Amplitude-frequency response and (b, d, f) Phase of the 1st, 2nd , and 3rd oscillators of the nonlinear discrete system, respectively.

3.2.1 Discrete MDOF Nonlinear System

The three-DOF nonlinear discrete system of Eq. (1) is used to verify the accuracy of the EDSM technique. The EDSM technique is used to identify various types of unknown internal forces including linear and nonlinear stiffnesses and linear damping, for both grounded and ungrounded cases.

For the purpose of verification, it is assumed that the response includes only the primary harmonic and simulation is performed accordingly. The effect of higher harmonics in the results of the identification is discussed later in the paper. Using the MCXA technique, described in Section 2.3, the steady state response of the system of Eq. (1) is obtained. Figure 7 gives the amplitude and phase of the response of the system, where the blue lines denote the stable responses and red lines show the unstable branches of the response of the system. The stability of the steady state response of the system was investigated using Lyapunov's first method of stability analysis.

Once the frequency domain response of the system has been obtained, the Equivalent Dynamic Stiffness Mapping technique is applied to identify the unknown internal forces of the system. The ideal equivalent dynamic stiffness of different types of internal forces are given in Table 1.

Accordingly, a linear spring and a cubic stiffness spring are shown respectively as a constant and a quadratic in the plot of the real part of the equivalent dynamic stiffness versus the amplitude of the response. On the other hand, linear damping is given as a constant in the plot of the imaginary part of the equivalent dynamic stiffness versus the amplitude of the response.

Figure 8 shows the real part of the equivalent dynamic stiffness in terms of the frequency domain amplitude of the response of the system. From the plot of the real part of D_{eq} the linear stiffness is identified as a constant, while the nonlinear part would be identified as a variation with respect to the amplitude of the response. Figure 8 (a) shows the grounded stiffness is composed of a linear and a nonlinear part which is attached to DOF 1. The ungrounded (connected) nonlinear stiffness between DOFs 2 and 3 is shown in Figure 8 (b). The grounded nonlinear stiffness attached to DOF 3 is shown in Figure 8 (c). The imaginary parts of the equivalent dynamic stiffness identify the equivalent damping coefficients of the nonlinear internal force, as shown in Figure 9. The grounded equivalent damping coefficients of DOFs 1 and 3 are linear in Figures 9 (a) and 9(b), respectively.

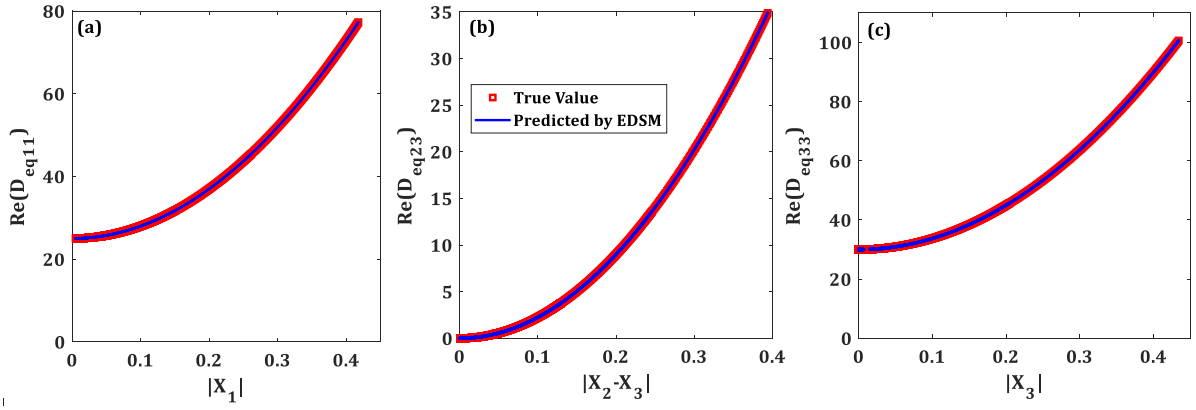

Figure 8- The real parts of the dynamic stiffness demonstrate the stiffness of nonlinear internal force of the system. (a) grounded nonlinear cubic stiffness including linear part at DOF1; (b) ungrounded nonlinear stiffness between DOFs 2 and 3; (c) grounded nonlinear stiffness including linear part connected to DOF 3.

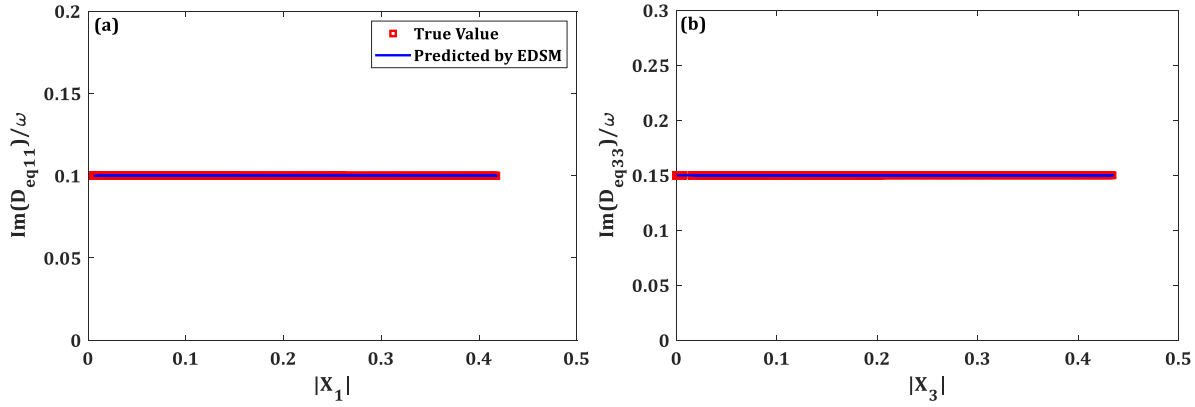

Figure 9- The imaginary parts of the dynamic stiffness identify the unknown linear damping at (a) DOF1 and (b) DOF 3.

3.2 Cantilever Beam

In order to investigate the capability of the EDSM identification technique in identifying the nonlinearities of continuous systems, a theoretical case study is carried out in this section on the cantilever beam described in Section 2.2. In order to verify the accuracy of the EDSM technique in the absence of all sources of inaccuracy, it assumed that there is no noise in the simulated data or modelling error in the underlying linear model. In addition, for the sake of simplicity, it is assumed that the response is free of higher harmonics. As the EDSM technique requires the response of the system to be given (simulated/measured) at all coordinates, in order to avoid any expansion error due to the estimation of unmeasured coordinates, the simulated response at all coordinates are utilized in the EDSM identification process. However, particularly for continuous systems, it is not possible to have complete measurements at all coordinates in practical applications.

The steady state dynamics of the cantilever beam is simulated by developing a code in MATLAB using the semi-analytical modified complex-averaging technique (MCXA) and are-length continuation [24, 25]. Different force amplitudes are applied to the beam in order to obtained the linear and nonlinear responses of the system. Figure 10 (a) illustrates the underlying linear and nonlinear responses of the system at DOF 11, the coordinate where the nonlinear restoring force is applied, for $F = 1$ N. To obtain the underlying linear system, the nonlinear element is neglected in the simulation. Figure 10 (b) shows the nonlinear response of the cantilever beam in the vicinity of first natural frequency for different values of force amplitude F.

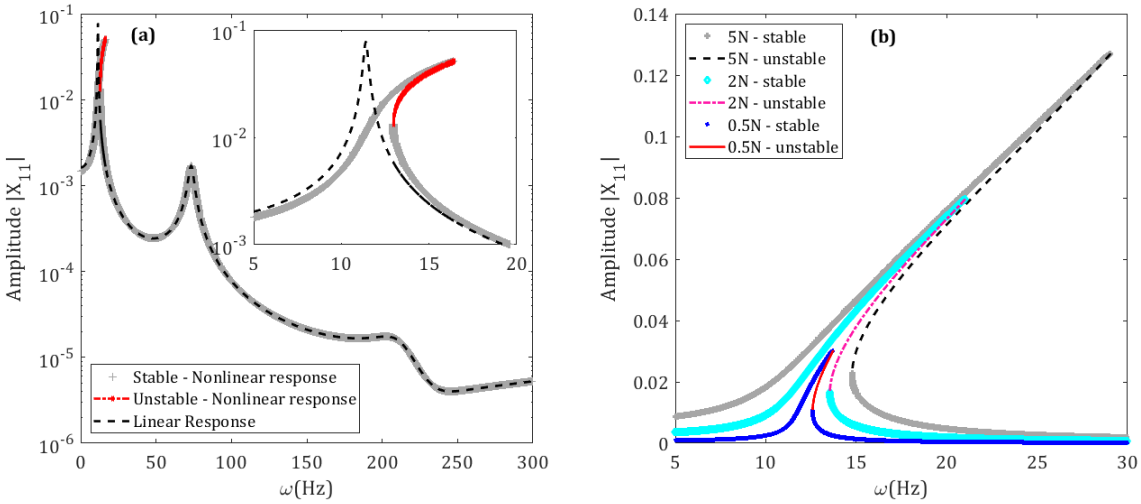

Figure 10- (a) Amplitude-frequency response of the underlying linear and nonlinear system of the cantilever beam for $F = 1\ N$; (b) amplitude-frequency response of the system for different force amplitudes.

From the nonlinear response of the system at all degrees of freedom, the Equivalent Dynamic Stiffness Mapping (EDSM) technique is used to identify the nonlinear element. Figures 11(a) and 11(b) respectively illustrate the comparison between the estimated and true values of the equivalent stiffness and damping of the nonlinear restoring force applied to the cantilever beam. Due to the Fourier Integral used to find the equations of motion in the frequency domain, the cubic nonlinear stiffness is given by a quadratic in Figure 11(a), with the constant $20\,\frac{\mathrm{N}}{\mathrm{m}}$ indicating the linear part of the stiffness. The nonlinear internal force also includes linear damping with $c_l =$

$0.004\frac{\text{N.s}}{\text{m}}$, and the identification gives an accurate constant value equal to the linear damping coefficient, see Fig. 11(b). As demonstrated, the EDSM technique is capable of accurately predicting the unknown nonlinear force, without any noise or error.

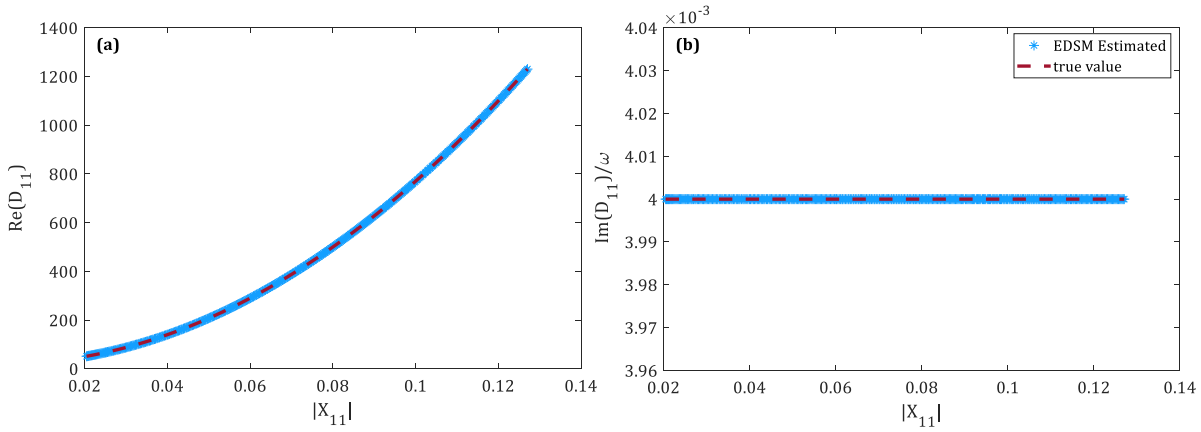

Figure 11- (a) Equivalent nonlinear stiffness, obtained from the real part of the equivalent dynamic stiffness, in comparison with the true value; (b) comparison of the estimated and true value of damping of the nonlinear restoring force.

4 Sensitivity to Error and Noise

Using the numerical simulation of both discrete and continuous nonlinear systems, the capability of the EDSM technique for the identification of nonlinearities has been investigated in the absence of noise and error. It is easy to avoid modelling errors and noise in simulated/measured data, but in practical systems and in experimental measurement, noise is inevitable in measured data. Therefore, having noise in the measured data makes it difficult to accurately identify the unknown elements/parameters and may lead to inaccuracy in the results of the identification.

In addition, many of the nonlinear identification methods require the underlying linear model to be properly updated in advance. However, since even the low amplitude response of a nonlinear system is not exactly same as the response of its underlying linear system, updating the underlying linear system using the measured response of the nonlinear system is unlikely to be free of error. This modelling error will also result in incorrect identification.

Incomplete measurement in experimental studies is considered as another source of error in the EDSM technique. Indeed, in practical systems, it is almost always impossible to have complete measurements due to insufficient equipment or sensors, or the difficulty in placing sensors. As the EDSM technique requires the responses of the system at all coordinates to be determined (measured or estimated), expansion methods are used to estimate the response at unmeasured DOFs, and this may create errors in the estimated data to be used in the EDSM technique.

The other source of error in the identification of nonlinear elements of dynamic structures is neglecting the presence of higher harmonics in the dynamics of the structure. Indeed, in many nonlinear structures the effect of higher harmonics in the response is too significant to be neglected. Therefore, utilizing only the primary harmonic of the response in the identification

process, as many of the identification methods do, may result in considerable error with respect to the magnitude of higher harmonics in the response.

In this section, the numerical simulations of the previously introduced continuous and discrete systems of the nonlinear cantilever beam and three-DOF Duffing oscillator are used to investigate the sensitivity of the EDSM technique to noise and various types of error such as expansion error, modelling error, and the error due to neglecting the higher harmonics in the response of nonlinear systems.

4.1 The Effect of Expansion Error

Expansion methods such as System Equivalent Reduction Expansion Process (SEREP) [1] are used to estimate the response of the system at unmeasured coordinates. For a system with p measured DOFs and q unmeasured DOFs, the unmeasured response is estimated using the SEREP method as

$$\begin{Bmatrix} \mathbf{X}_m \\ \mathbf{X}_u \end{Bmatrix} = \mathbf{T}\mathbf{X}_m, \tag{19}$$

where $[\mathbf{X}_m]_{p\times 1}$ **and** $[\mathbf{X}_u]_{q\times 1}$ are respectively the measured response and estimated response at unmeasured coordinates, $[\mathbf{T}]_{\mathbf{n}\times\mathbf{m}}$ denotes the transform matrix of the SEREP method, and n is the number of total degrees of freedom. Since such expansion methods are usually based on the linear systems, using them for nonlinear systems may lead to some error in the estimated response. Therefore, the estimated response at unmeasured coordinates is slightly deviated from the actual unmeasured response, $\mathbf{X}_u = \mathbf{X}_u^a + \delta\mathbf{X}_u$. $\mathbf{X}_u^a$ is the actual response at unmeasured DOFs and $\delta\mathbf{X}_u$ denotes the error of estimating the response at unmeasured DOFs using SEREP. Nonlinear force may be obtained using the estimated response as

$$\begin{gathered} \mathbf{F}_{NL} = \mathbf{F}_{ex} - (\mathbf{K} + j\omega\mathbf{C} - \omega^2\mathbf{M})\left(\begin{Bmatrix} \mathbf{X}_m \\ \mathbf{X}_u^a \end{Bmatrix} + \begin{Bmatrix} \mathbf{0} \\ \delta\mathbf{X}_u \end{Bmatrix}\right), \\ \mathbf{F}_{NL} = \mathbf{F}_{NL}^a + \delta\mathbf{F}_{NL} \end{gathered} \tag{20}$$

where $\mathbf{F}_{NL}^a$ denotes the vector of actual nonlinear force and $\delta\mathbf{F}_{NL}$ is the vector of error in the identified nonlinear force arising from the use of SEREP method to estimate the response at unmeasured coordinates.

$$\delta\mathbf{F}_{NL} = -(\mathbf{K} + j\omega\mathbf{C} - \omega^2\mathbf{M})\begin{Bmatrix} \mathbf{0} \\ \delta\mathbf{X}_u \end{Bmatrix} \tag{21}$$

To study the effect of expansion error, it is assumed that the measurements on the beam are carried out on only three degrees of freedom (DOFs 1, 5, 9) using three simulated accelerometers shown in Figure 2. Hence, the responses of the measured coordinates are expanded using the SEREP expansion method [1] to predict the response at unmeasured DOFs. Figure 12 (a) shows the measured and estimated responses for the translational coordinates of the system under 1N harmonic excitation force in the neighbourhood of first natural frequency. The expansion error from the SEREP expansion is given in Figure 12 (b). The maximum expansion error for the translational DOFs is 1.5% at DOF11. The EDSM technique is then applied to the simulated (DOFs

1, 5, 9) and estimated (other DOFs) steady state response of the system obtained for different amplitudes of external force, F, to identify the unknown nonlinear elements.

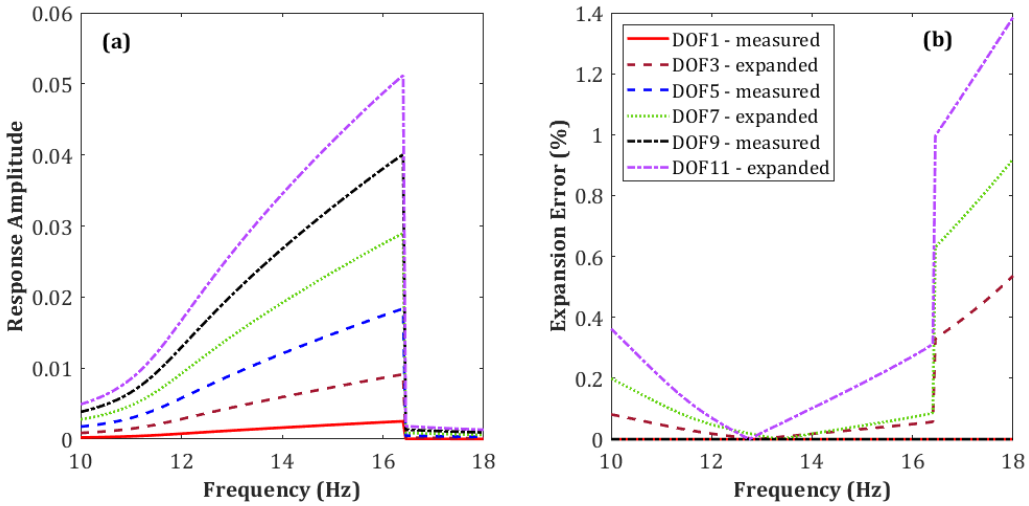

Figure 12- (a) Estimation of the translational responses of the system at unmeasured DOFs using the measured data and SEREP expansion. (b) The expansion error (%) for translational DOFs.

Applying the SEREP expansion method to the incomplete measurement, identified stiffness and damping gives the results shown in Figure 13. To fit a curve to the EDSM data, a constant function for the linear damping and a quadratic curve for the nonlinear cubic stiffness are assumed. The identified nonlinear force is given as,

$$F_N = c_l \dot{w}(l,t) + k_l w(l,t) + k_N w(l,t)^3,$$
$$c_l = 0.0435 \frac{\text{N.s}}{\text{m}}, \qquad k_l = 40 \frac{\text{N}}{\text{m}}, \qquad k_N = 7.3 \times 10^4 \frac{\text{N}}{\text{m}^3}. \tag{22}$$

The error caused by the expansion has led to errors of 987%, 100%, and 27% in the identification of c_l, k_l, and k_N, respectively.

The identification process has been performed using different numbers of coordinates of the simulated response of the system to study the effect of expansion error in the final results of the identification. Figure 14 demonstrates how increasing the number of measured/simulated coordinates may decrease the level of error in the results of the identification.

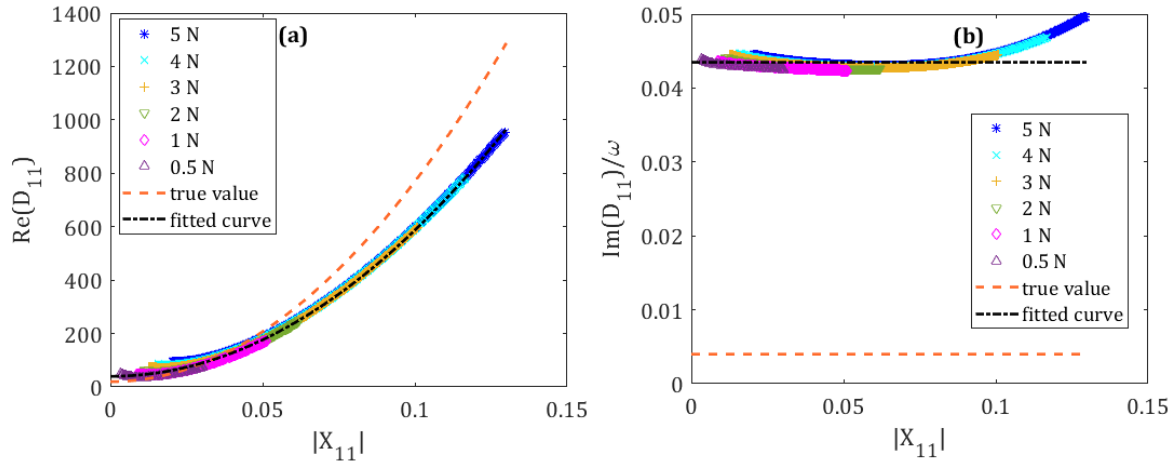

Figure 13- Errors in the identified stiffness (a) and damping (b) due to using SEREP expansion to estimate the response at unmeasured DOFs. The response was simulated/measured only at three DOFs: 1, 5, and 9.

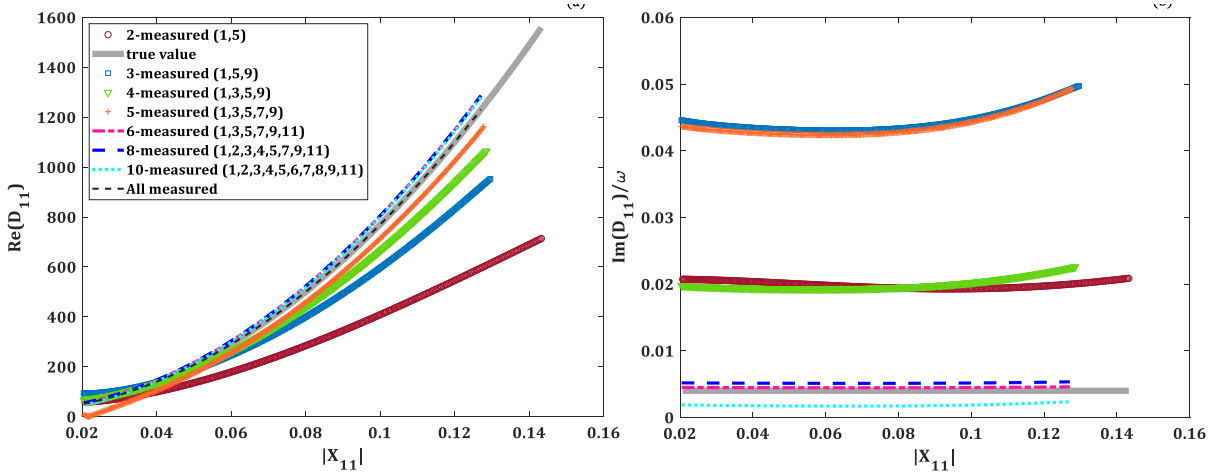

Figure 14- Identification of the unknown nonlinear force using the simulated response at different numbers of degrees of freedom. The response of the system was obtained for $F = 4\ N$.

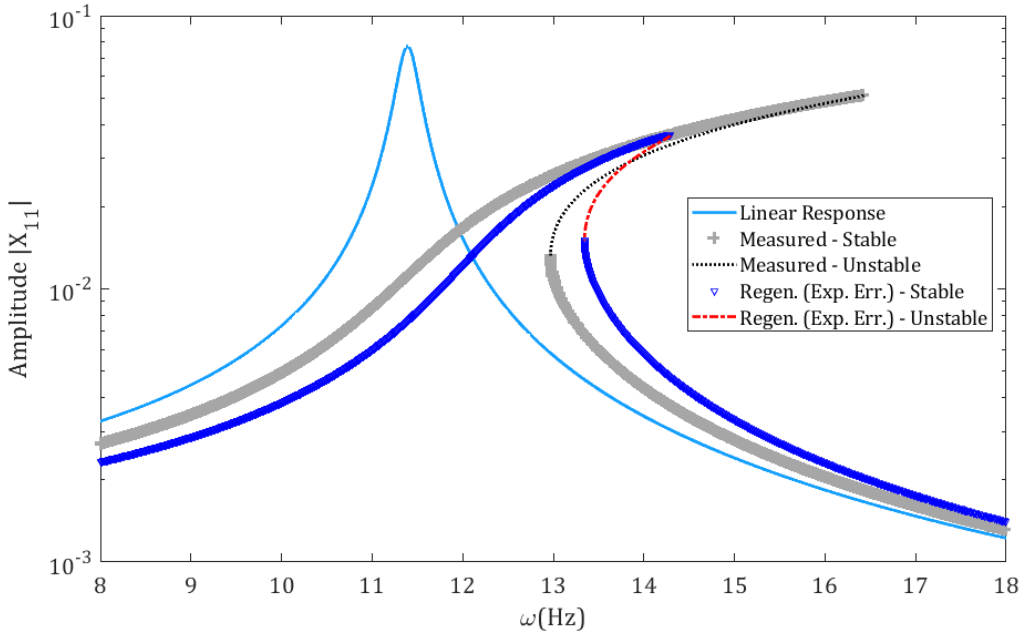

Figure 15- Comparison of the simulated response of the nonlinear system with the response regenerated using the identified parameters of Eq. (22), considering the effect of expansion error.

The main purpose of the identification of nonlinear systems is to generate an accurate mathematical model so that it can predict the behaviour of the system precisely. Figure 15 shows a comparison between the simulated response of the nonlinear system and the response regenerated using the identified nonlinear force of Eq. (22). It is observed that the identified parameters are not able to regenerate exactly the simulated response.

4.2 The Effect of Modelling Error

Other than the error due to the expansion of the incomplete measured responses, modelling error may result in considerable error in the identified parameters. Modelling error comes from updating the underlying linear system and it may arise from contaminated data or using the low amplitude nonlinear response to identify the underlying linear model. Having modelling error in the updated underlying linear model is shown by deviation from actual values of the linear system as

$$\mathbf{M} = \mathbf{M}^{a} + \boldsymbol{\delta}\mathbf{M}, \qquad \mathbf{C} = \mathbf{C}^{a} + \boldsymbol{\delta}\mathbf{C}, \qquad \mathbf{K} = \mathbf{K}^{a} + \boldsymbol{\delta}\mathbf{K}, \tag{23}$$

where $\mathbf{M}, \mathbf{C}$, and $\mathbf{K}$ are respectively updated mass, damping, and stiffness matrices. Superscript $\blacksquare^{a}$ and $\boldsymbol{\delta}$ denote the actual value and error of each identified matrix, respectively. Using an inaccurate underlying linear model may lead to inaccurate nonlinear force as

$$\mathbf{F}_{NL} = \mathbf{F}_{ex} - \left(\mathbf{K}^{a} + \boldsymbol{\delta}\mathbf{K} + j\omega(\mathbf{C}^{a} + \boldsymbol{\delta}\mathbf{C}) - \omega^{2}(\mathbf{M}^{a} + \boldsymbol{\delta}\mathbf{M})\right)\left(\begin{Bmatrix}\mathbf{W}_{m}\\ \mathbf{W}_{u}^{a}\end{Bmatrix} + \begin{Bmatrix}\mathbf{0}\\ \delta\mathbf{W}_{u}\end{Bmatrix}\right),$$
$$\mathbf{F}_{NL} = \mathbf{F}_{NL}^{a} + \delta\mathbf{F}_{NL} \tag{24}$$

where $\mathbf{F}_{NL}^{a}$ denotes the vector of actual nonlinear force and $\delta\mathbf{F}_{NL}$ is the vector of error in the identified nonlinear force arising from the use of SEREP method to estimate the response at unmeasured coordinates and modelling error in updating the underlying linear system.

$$\delta\mathbf{F}_{NL} = -(\mathbf{K}^{a} + j\omega\mathbf{C}^{a} - \omega^{2}\mathbf{M}^{a})\begin{Bmatrix}\mathbf{0}\\ \delta\mathbf{W}_{u}\end{Bmatrix} - (\boldsymbol{\delta}\mathbf{K} + j\omega\boldsymbol{\delta}\mathbf{C} - \omega^{2}\boldsymbol{\delta}\mathbf{M})\left(\begin{Bmatrix}\mathbf{W}_{m}\\ \mathbf{W}_{u}^{a}\end{Bmatrix} + \begin{Bmatrix}\mathbf{0}\\ \delta\mathbf{W}_{u}\end{Bmatrix}\right) \quad (25)$$

A usual way to update the underlying linear system is using the response of the nonlinear system excited by a very low-amplitude external force. Although the effect of nonlinear force on the response of the system decreases by reducing the amplitude of excitation force, one cannot get rid of it in practical systems. In other words, one of the most significant sources of modelling error is the difference between the response of the true (pure linear) underlying linear system and the linear response obtained from a low amplitude excitation test of the nonlinear system. A low amplitude excitation of 0.01 N was applied to both the underlying linear system and the nonlinear system of Figure 2 and the responses are shown in Figure 16. Such differences in the responses may cause errors in updating the modal parameters of the underlying linear system (i.e. natural frequency, damping ratio, and mode shape). As the updated underlying linear model of the nonlinear system is used for both expansion and identification, the existence of modelling errors may lead to additional errors in both the expansion and the identification of the system.

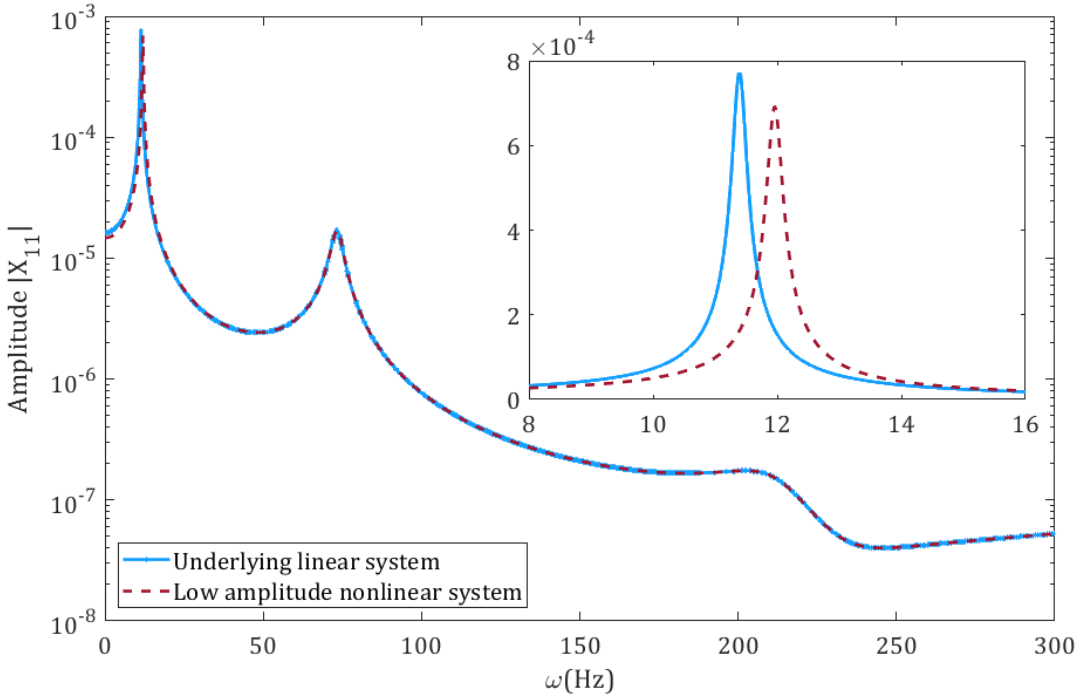

Figure 16- Difference between a purely linear system and the response of a nonlinear system with a very low amplitude excitation.

Here it is assumed that a complete measurement has been performed and there is no expansion error in the identification process. Figure 17 demonstrates the identification of the unknown internal stiffness and damping considering two levels of modelling error $(+5\%, +10\%)$ in the parameters of the underlying linear system (E, ρ, γ). Applying 5% and 10% modelling error to

the parameters of the underlying linear system resulted in 5% and 9% errors in the identification of the nonlinear stiffnesses, respectively. The errors for the identified linear stiffnesses were 5% and 12.5%. Furthermore, EDSM was not capable of estimating the linear damping. The identified nonlinear forces for two levels of modelling error were obtained as,

$$F_N = c_l\dot{w}(l,t) + c_N\dot{w}(l,t)w(l,t)^2 + k_l w(l,t) + k_N w(l,t)^3, \tag{26}$$

#modelling error of +5%,

$$c_l = 0.0034\frac{\text{N.s}}{\text{m}}, \qquad c_N = 0.325\frac{\text{N.s}}{\text{m}^3}, \qquad k_l = 19\frac{\text{N}}{\text{m}}, \qquad k_N = 1.05\times 10^5\frac{\text{N}}{\text{m}^3}. \tag{27}$$

#modelling error of +10%,

$$c_l = 0.0028\frac{\text{N.s}}{\text{m}}, \qquad c_N = 0.675\frac{\text{N.s}}{\text{m}^3}, \qquad k_l = 17.5\frac{\text{N}}{\text{m}}, \qquad k_N = 1.09\times 10^5\frac{\text{N}}{\text{m}^3}. \tag{28}$$

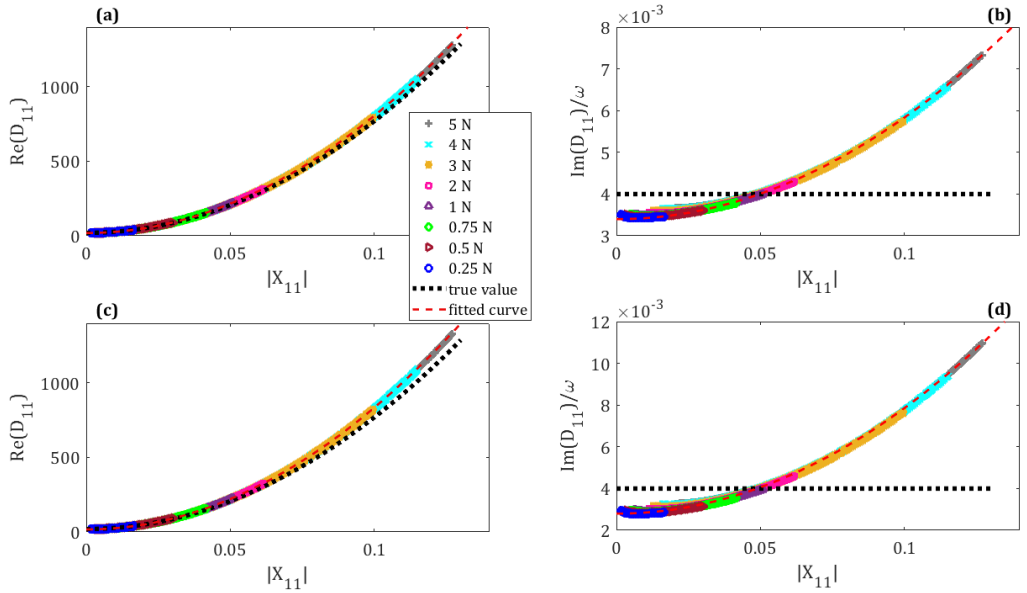

Figure 17 - The effect of modelling error on the identification of nonlinear force of the system using the EDSM method. (a & b) modelling error of +5% (c & d) modelling error of +10%.

4.3 The Effect of Noise

Figures 18 and 19 show the effect of noise in the measured data on the results of the identification. In order to investigate the effect of noise, four different levels $(0.5, 1, 2, 5\ \%)$ of normally distributed noise have been applied to the response of the system. Incomplete measurements are assumed and there is no modelling error. In fact, a combination of expansion error and noise effects are shown in Figures 18 and 19. It is observed in Figure 18 that increasing the noise level in the response of the system may make it difficult to fit a reasonable curve to the EDSM data

points, and therefore, it would be difficult to identify the nonlinear internal force. Note that, in practice, the noise is not likely to be normally distributed.

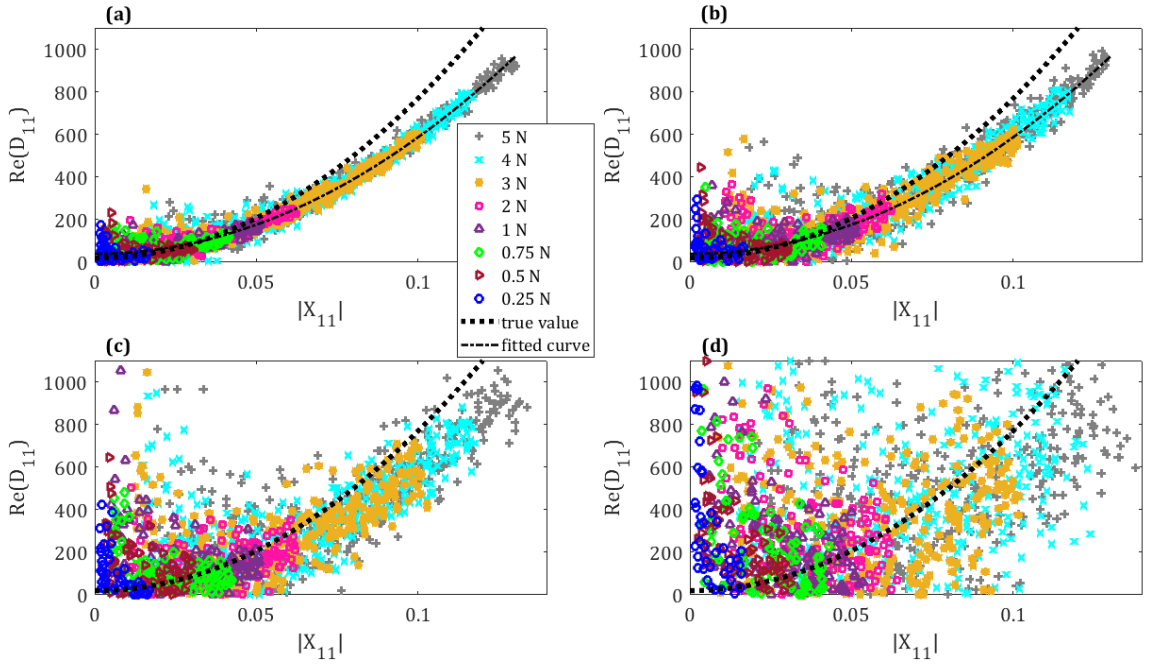

Figure 18- Identification of stiffness with different noise levels. (a) 0.5%, (b) 1%, (c) 2%, (d) 5%.

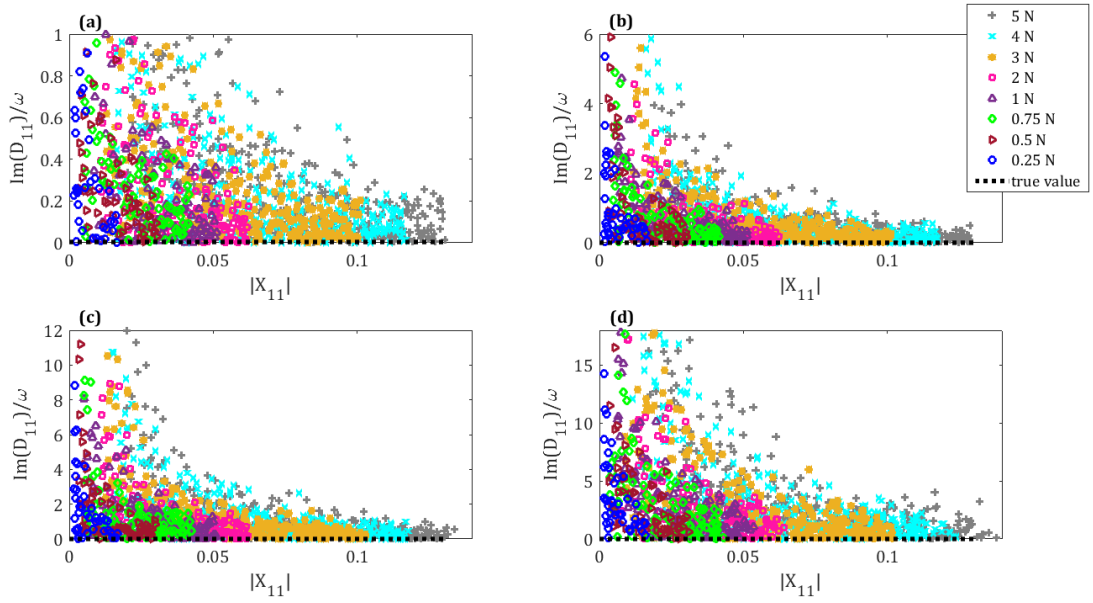

Figure 19- Identification of damping with different noise levels. (a) 0.5%, (b) 1%, (c) 2%, (d) 5%.

4.4 The Effect of Higher Harmonics

One of the most important problems to be considered in the analysis of nonlinear systems is the participation of the higher harmonics in the response of the system. Although the primary harmonic is dominant in many nonlinear systems and higher harmonics can be neglected during the analysis, neglecting higher harmonics in cases where they play a significant role in the behaviour of the system may lead to considerable errors in the results of the analysis. In this section, the effect of higher harmonics on the results of identification of nonlinear elements of dynamical systems is investigated. To this end, the 3 DOF discrete system of Figure 1 is considered.

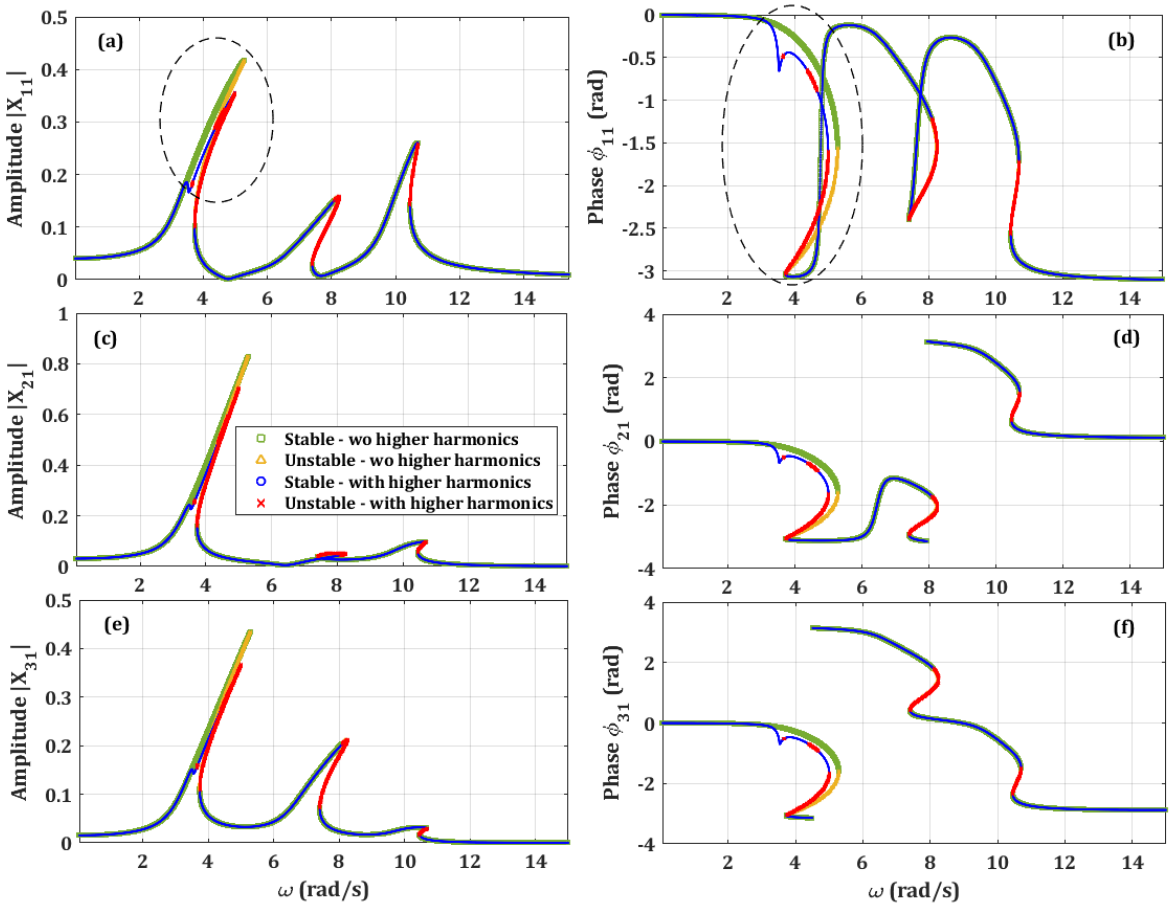

Figure 20- Comparison of the primary harmonic of the nonlinear response of the three-DOF discrete system with and without considering higher harmonics in the simulation.

The simulated steady state dynamics of the system shown in Figure 7 was obtained neglecting the higher harmonics in the response, and the parameters were identified in Figures 8 and 9 based on this assumption. However, higher harmonics usually play significant role in the dynamics of nonlinear systems. The simulation data was used to identify the unknown nonlinear elements of the system, and the response was assumed to include only the primary harmonic. Therefore, neglecting higher harmonics in the identification process would not lead to an effective identification. In this section, the higher harmonics are considered in the response of the system and it is assumed that the simulation/measurement includes higher harmonics in addition to the primary harmonics in the steady state response of the system.

Figure 20 illustrates the amplitude and phase of the primary harmonic of the response of the nonlinear system in the frequency domain, with and without the presence of higher harmonics in the simulation. $|X_{11}|$, $|X_{21}|$, and $|X_{31}|$ in Figure 20 denote the amplitudes of the primary harmonics of three degree of freedom of the system of Figure 1, respectively. φ_{11}, φ_{21}, and φ_{21} represent the phases of the primary harmonic of the steady state response of the 3DOF system. As shown, the presence of higher harmonics makes the most difference for the first resonant frequency of the response. And among all three degrees of freedom, DOF 1 has been affected more than two other DOFs. The amplitude and phase of the first three harmonics of the response of the nonlinear system of Eq. (14) is shown in Figure 3. The phase of the response of each degree of freedom is the same for all harmonics. As shown, due to the presence of the cubic nonlinearity in the system, the amplitude of the second harmonic is zero as expected. However, the third harmonic of the response mainly appears in the vicinity of the first resonant frequency, and its amplitude is small in the neighbourhood of the second and third resonances. The maximum ratio between the amplitude of the third harmonics of the response of DOF 1 and the amplitude of its primary harmonic is 0.5 at $\omega = 3.53$ (rad), while this ratio is 0.14 at $\omega = 3.53$ (rad) for DOF 2 and 0.09 at $\omega = 5$ (rad) for DOF 3. All of these peak points occur within the neighbourhood of the first resonance, $\omega = 2 - 6$ (rad). Accordingly, neglecting the higher harmonics in the response of the system in the vicinity of first resonant frequency has the biggest effect in generating errors in the identification. In other words, implementing the identification process using only the primary harmonic of the response within the frequency range of the second and third resonances, as illustrated in Figures 21 and 22, may not lead to significant errors in the results, as the higher harmonics cannot be observed strongly in the response in that region. Figures 21 and 22 demonstrate the results of the identification of the unknown parameters using the primary harmonic of the response of the system within the region of the second and third resonances, respectively. Apparently, due to the small participation of the higher harmonics in these regions, the magnitude of the error in the identification is not significant. In contrast, if the identification is performed using only the primary harmonic of the response in the vicinity of the first resonance, neglecting higher harmonics will result in significant errors in the identification results, see Figure 23. In Figures 21-23, $|X_{11}|$, $|X_{21}|$, and $|X_{31}|$ are, respectively, the amplitudes of the primary harmonics of three degrees of freedom of the system of Figure 1. $D_{eq_{11}}$, $D_{eq_{11}}$, $D_{eq_{11}}$ denote the equivalent dynamic stiffness, respectively, for the grounded nonlinear element attached to DOF 1, the ungrounded nonlinear force between DOFs 2 and 3, and the grounded nonlinear element attached to DOF 3.

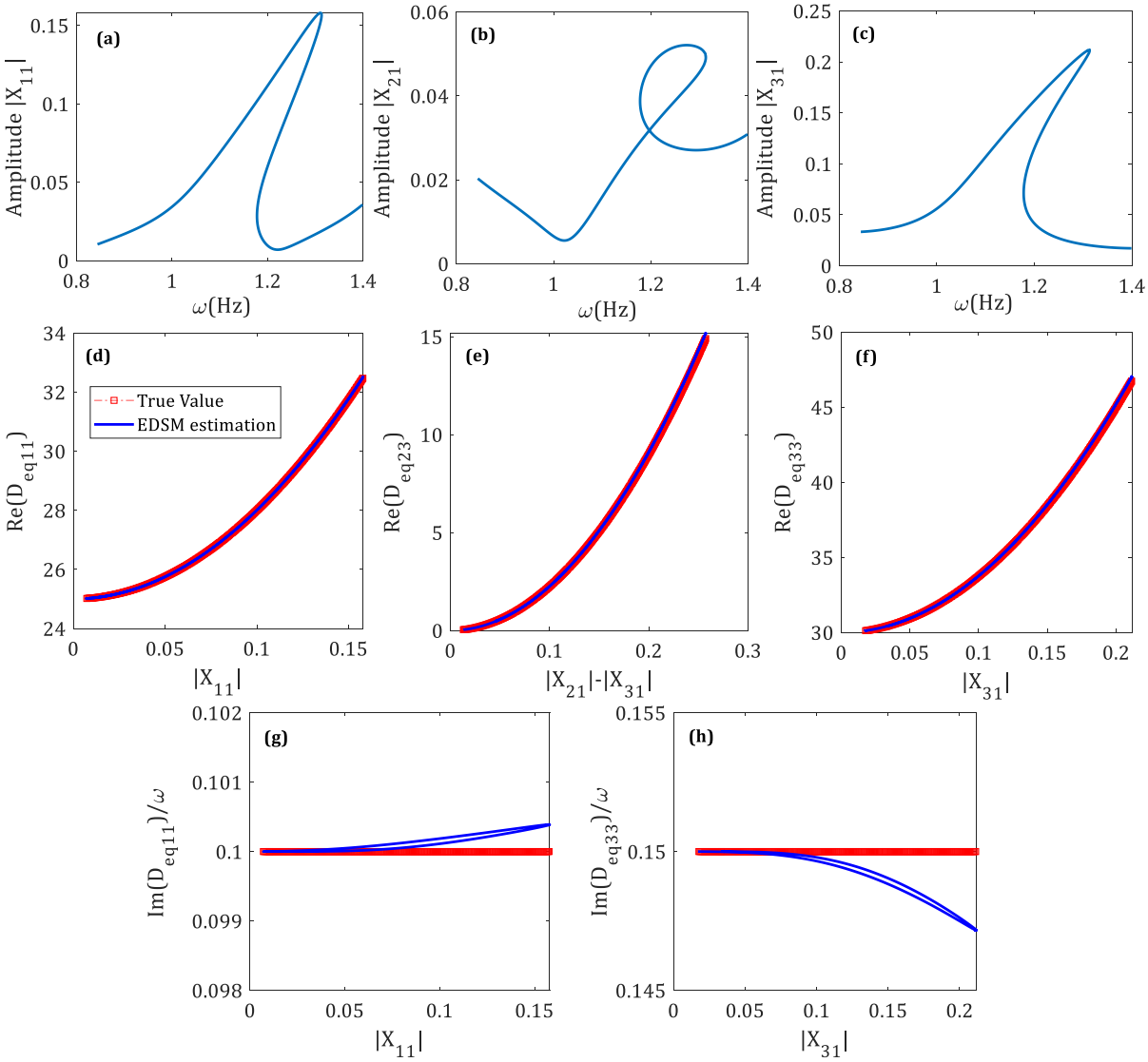

Figure 21- (a, b, c) The primary harmonic of the amplitude-frequency responses of three oscillator in the neighbourhood of second resonance used in the EDSM identification; (d, e, f) Comparison of true EDSM-estimated nonlinear stiffnesses and linear damping (g and h).

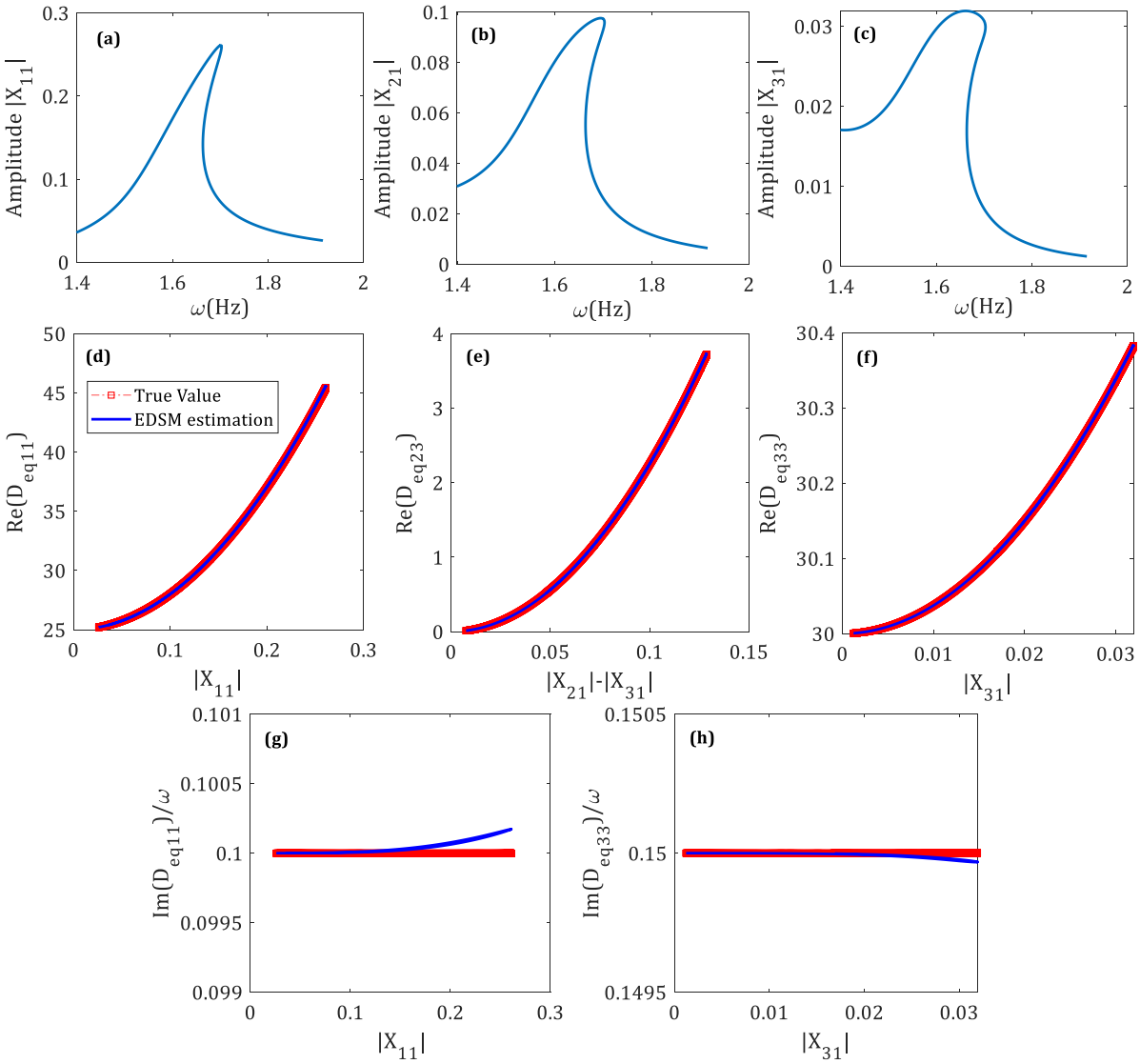

Figure 22- (a, b, c) The primary harmonic of the amplitude-frequency responses of three oscillator in the neighbourhood of third resonance used in the EDSM identification; (d, e, f) Comparison of true EDSM-estimated nonlinear stiffnesses and linear damping (g and h).

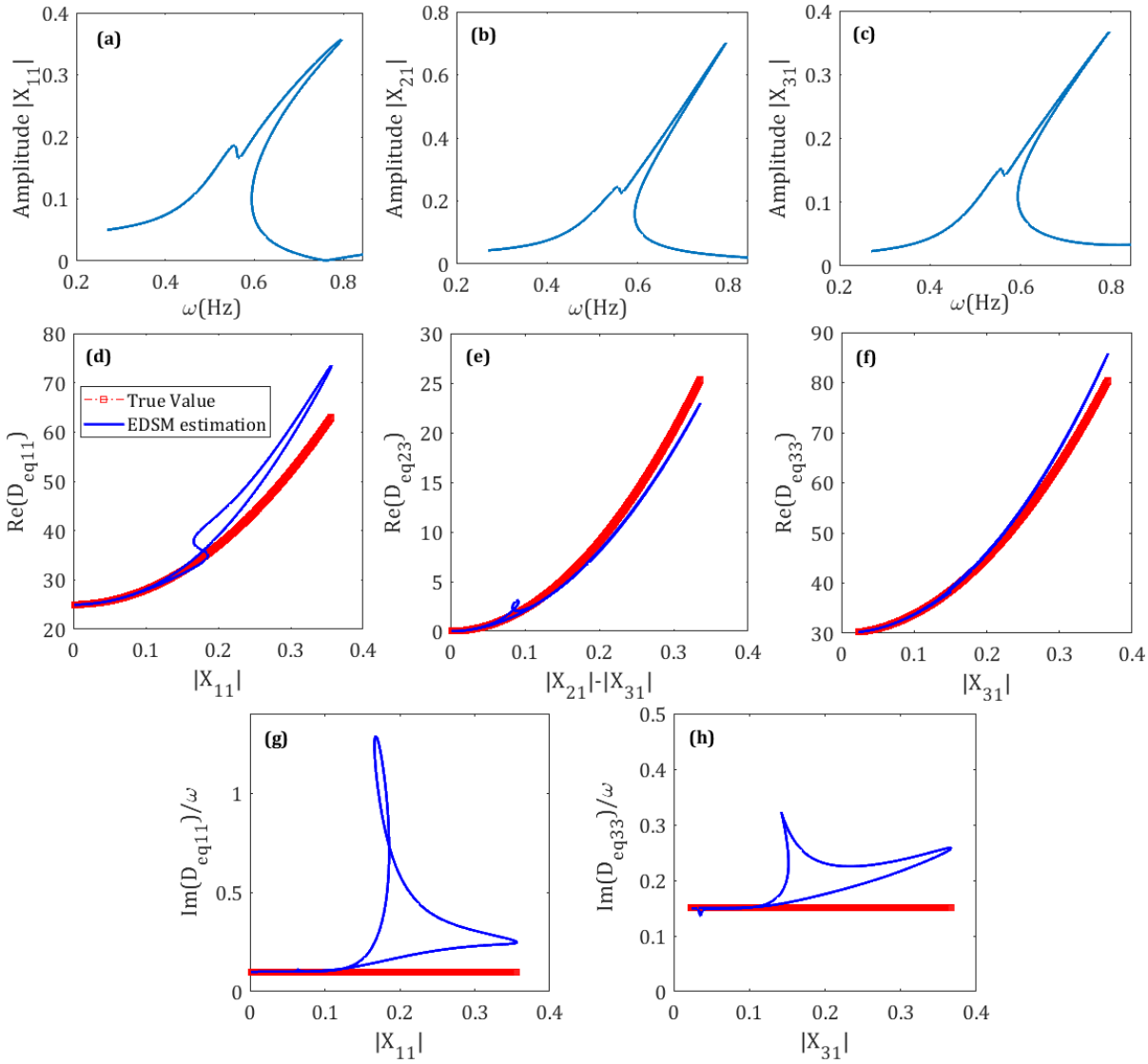

Figure 23- (a, b, c) The primary harmonic of the amplitude-frequency responses of three oscillator in the neighbourhood of first resonance used in the EDSM identification; (d, e, f) Comparison of true EDSM-estimated nonlinear stiffnesses and linear damping (g and h).

5 Identification Using Optimization

According to the discussion in Section 4, one may conclude that there are many sources of inaccuracy affecting the results of identification methods, particularly for the EDSM technique. To avoid such sources of inaccuracy, or at least to reduce their effects on the results of identification, Taghipour et al. [22] proposed an optimization-based framework to identify nonlinear structures. In this section, the nonlinear system of the cantilever beam of Figure 2 is identified utilizing the framework proposed in [22]. For this purpose, following assumptions and considerations are taken into account:

- Only the inaccuracy due to expansion method is considered. All other sources of inaccuracy (i.e. noise and modelling error) are neglected.

- The identified nonlinear force obtained from the EDSM method are considered as the initial estimate for the unknown parameters of the nonlinear force in the optimization process.
- The objective function is defined so that the difference between the measured/simulated and estimated nonlinear response are minimized.

$$J = \min\left(\sum_{i=1}^{N_f} |\log(\|X_m(\Omega_i)\|_2) - \log(\|X_a(\Omega_i)\|_2)|\right), \tag{29}$$

where X_m and X_a are respectively the experimental/simulated response and the estimated response of the system in the frequency domain.

- Considering the response of the system in the vicinity of the resonance may improve the efficiency of the optimization process.
- In nonlinear systems, multiple solutions for the response may occur (more than one stable solution). In such cases, the most significant stable branch of the response is considered within the range of the multiple solutions.
- The unstable solution of the numerical estimation is neglected, as it is almost impossible to measure the unstable solution in an experiment.

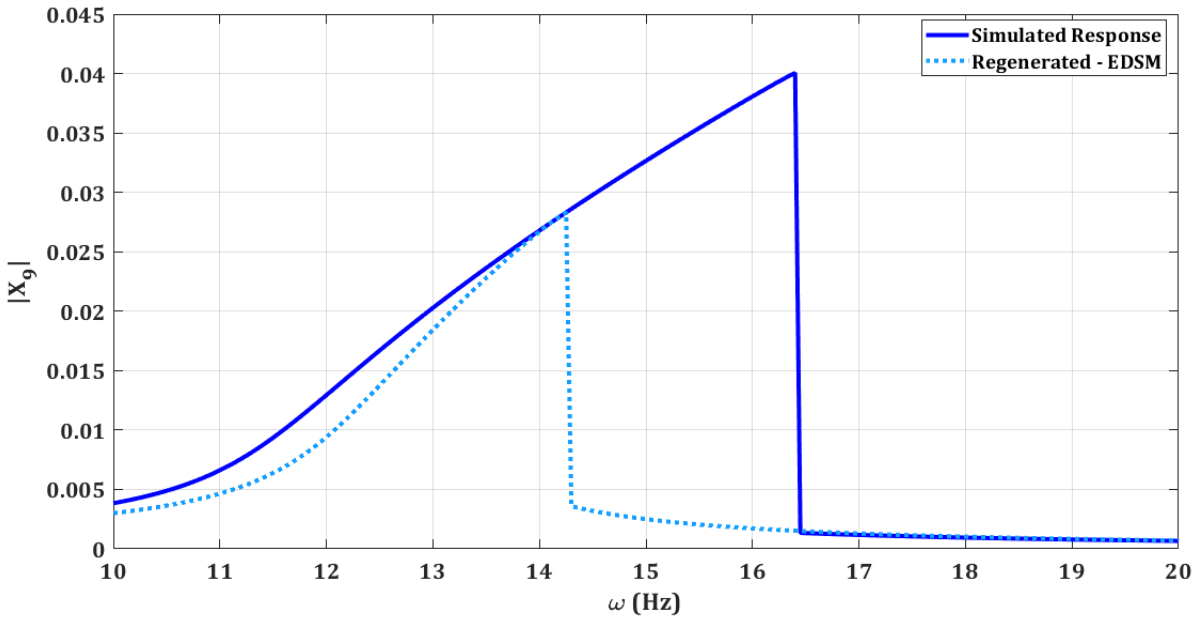

Figure 24- Simulated/measured response at DOF 9 compared with the regenerated response obtained from the nonlinear model identified using EDSM technique.

To compare the result of the optimization-based framework with the result of the EDSM technique, the identified nonlinear force of the cantilever beam given by Eq. (22) is considered as the initial estimate for the optimization process. It is assumed that the response of the cantilever beam is measured at only the three DOFs 1, 5, and 9. Figure 24 shows the simulated response at DOF 9 of the beam under the excitation force amplitude of $F = 1$ N and compares it with the regenerated response obtained using the identified nonlinear force from the EDSM technique. As mentioned above, the unstable and the lower stable branch of the response are neglected. The optimization method aims to minimize the difference between the simulated/measured and the

estimated response. As a spatially complete measurement is not required in the optimization-based framework, it is not necessary to use an expansion method in order to estimate the response at unmeasured DOFs. Therefore, the measured response at only one of the measured DOFs (e.g. DOF 9) is used for the optimization process. The optimized parameters of the nonlinear force are obtained using the optimization process exploiting the identified parameters of Eq. (22) as the initial estimate. Table 4 gives a comparison between the true values of the parameters of the nonlinear force and the identified values obtained from the EDSM and optimization methods.

Table 4- Optimized parameters of the nonlinear force of the cantilever beam.

Parameters (unit)	True value	Identified by EDSM		Optimized	
		value	Error (%)	value	Error (%)
c_l $(\frac{\text{N.s}}{\text{m}})$	0.004	0.0435	987	0.00427	6.75
k_l $\left(\frac{\text{N}}{\text{m}}\right)$	20	40	100	21.586	19.93
k_N $\left(\frac{\text{N}}{\text{m}^3}\right)$	1×10^5	7.3×10^4	-27	9.355×10^4	-6.45

As it can be seen, the accuracy of the identified values of the parameters have been significantly improved. However, as the cubic stiffness is dominant in dynamics of the system at the vicinity of the resonant frequency, the linear stiffness has not been optimized to a very accurate value. The optimized parameters are used to regenerate the nonlinear response of the cantilever beam. Figure 25 compares the simulated nonlinear response with the numerically regenerated ones obtained from the nonlinear models identified using the EDSM technique and the optimization method. The identified nonlinear model obtained from optimization method is shown to be more accurate than the identified model of the EDSM technique.

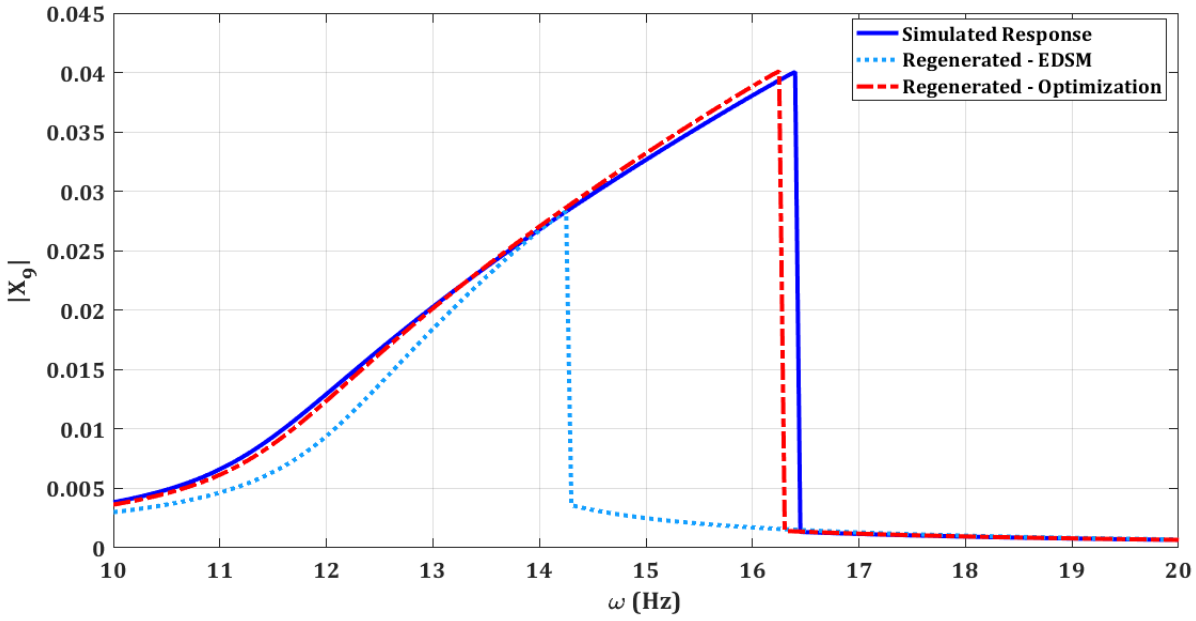

Figure 25- Simulated/measured response at DOF 9 compared with the regenerated response obtained from nonlinear models identified using the EDSM technique and the optimization-based framework.

To verify the reliability of the model identified using the optimization-based framework, the simulated/measured responses of the system at three measured, namely DOFs 1, 5, and 9, are compared with the regenerated response using the optimized parameters. Figure 26 illustrates the comparison between the simulated and regenerated response at DOFs 1, 5, and 9. Although the optimization was performed using only DOF 9, the identified model is capable of estimating the response at the other degrees of freedom.

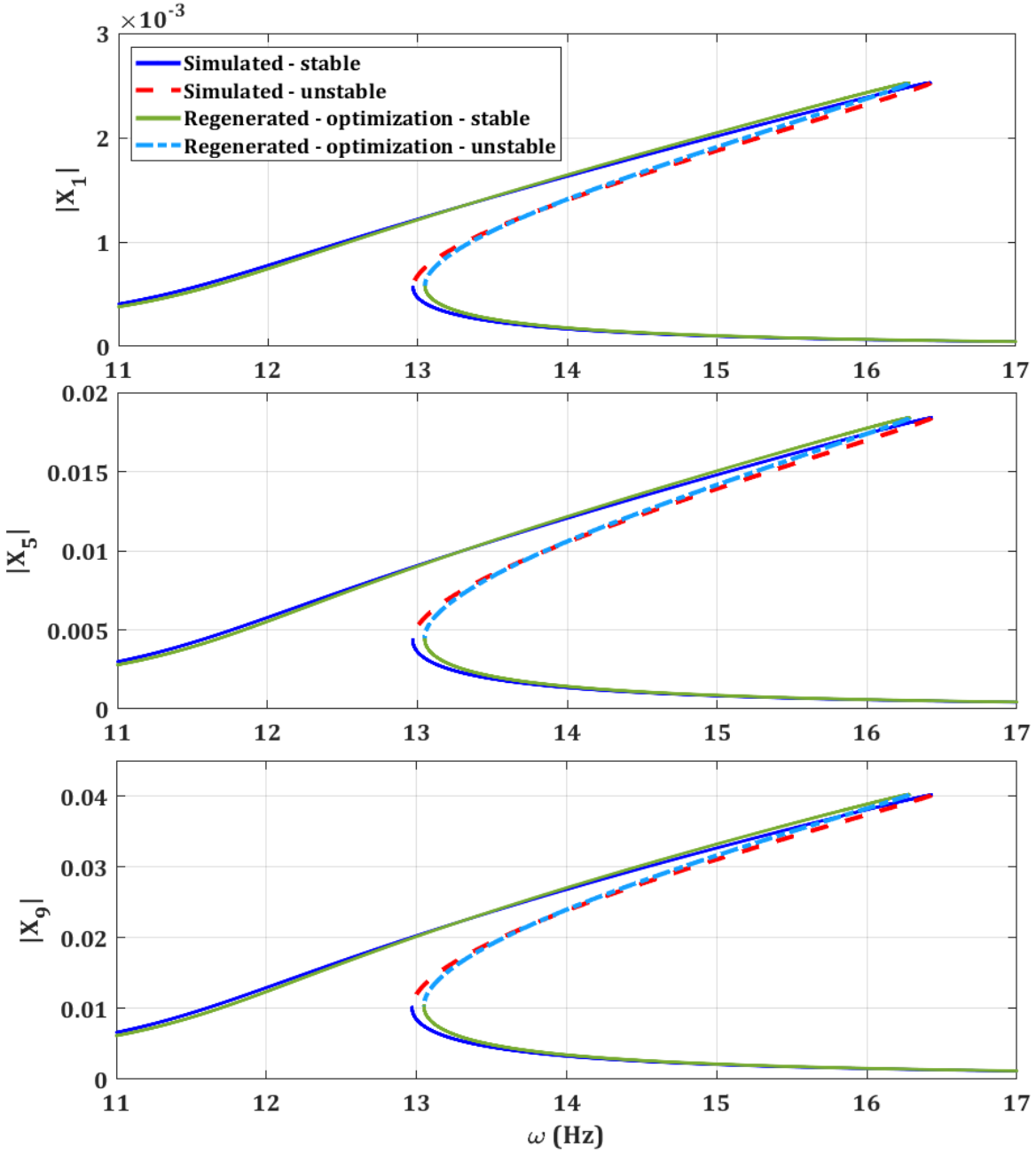

Figure 26- Comparison between the simulated/measured response at DOFs 1, 5, and 9 and the regenerated response obtained from nonlinear model identified using the optimization method.

6 Conclusion

This paper has investigated the sensitivity of the identification using the Equivalent Dynamic Stiffness Mapping (EDSM) technique to noise in measured data and various types of error such as expansion error, modelling error, and the error due to neglecting the higher harmonics in the response of nonlinear systems. For this purpose, a theoretical study has identified the structural nonlinearities of two nonlinear systems (a discrete three-DOF Duffing system and a cantilever beam with a nonlinear restoring force applied to the tip of the beam) considering the presence of all the aforementioned sources of inaccuracy (noise and error). First, the accuracy of the EDSM technique in the identification of nonlinear elements has been verified by applying the method to two example nonlinear systems. Afterwards, numerical simulation of the two systems has been performed in MATLAB and the simulated data has been used to investigate the effect of the presence of noise in the simulated/measured data, expansion error in the estimation of the unmeasured coordinates, modelling error in the updated underlying linear model, and the error due to neglecting the higher harmonics in the nonlinear response of the system, on the outcome of the identification process. The nonlinear response of the system has been regenerated using the identified parameters with the presence of the sources of error and the generated response was compared with the simulated response in the absence of any noise or error. According to the results, although the EDSM technique is capable of identifying accurately the nonlinear elements in the absence of any source of inaccuracy, it has been demonstrated that this method is very sensitive to sources of inaccuracy and would result in significant errors in the model of the nonlinear system. Finally, the nonlinear force of the system with a cantilever beam was identified utilizing an optimization framework using the results of EDSM technique as the initial parameter estimate for the optimization process. Minimizing the difference between the measured/simulated and estimated nonlinear responses of the system at one of the measured coordinates was set as the objective function of the optimization process. The validity of the results of the optimization method was verified by comparing the response at other measured DOFs. Using the optimization method, one may avoid the inaccuracy resulting from expansion methods or the effect of higher harmonics. The comparison between the estimated and measured responses illustrates that the optimization method is able to identify the nonlinear system and regenerate the measured/simulated nonlinear response.

Acknowledgement

The authors acknowledge the financial support from the Engineering and Physical Sciences Research Council, through grant numbers EP/R006768/1, EP/S017925/1 and EP/P01271X/1. Javad Taghipour gratefully acknowledges the financial support from College of Engineering at Swansea University.

References

[1] M.I. Friswell, J.E. Mottershead, *Finite Element Model Updating in Structural Dynamics*, Springer Science & Business Media (1995).

[2] J.E. Mottershead, M. Link, M.I. Friswell, *The sensitivity method in finite element model updating: a tutorial*, Mechanical Systems and Signal Processing, Vol. 25, No. 7, (2011), pp. 2275–2296.

[3] D.J. Ewins, *Modal Testing: Theory, Practice.*, Research studies press, Letchworth (1995).

[4] N.M.M. Maia, J.M.M. Silva, Theoretical and experimental modal analysis, Research Studies Press, Baldock, United Kingdom (1997).

[5] K. Worden, G. Tomlinson, *Nonlinearity in Structural Dynamics: Detection, Identification and Modelling,* Philadelphia, IOP Publishing Ltd., Bristol (2001).

[6] G. Kerschen, K. Worden, A.F. Vakakis, J. Golinval, *Past, present and future of nonlinear system identification in structural dynamics,* Mechanical Systems and Signal Processing, Vol. 20, No. 3, (2006), pp. 505-592.

[7] J.P. Noël, G. Kerschen, *Nonlinear system identification in structural dynamics: 10 more years of progress,* Mechanical Systems and Signal Processing, Vol. 83, (2017), pp. 2-35.

[8] C.M. Cheng, Z.K. Peng, W.M. Zhang, G. Meng , *Volterra-series-based nonlinear system modeling and its engineering applications: A state-of-the-art review,* Mechanical Systems and Signal Processing, Vol. 87, (2017), pp. 340-364.

[9] Z.C. Wang, W.X. Ren, G. Chen, *Time–frequency analysis and applications in time-varying/nonlinear structural systems: A state-of-the-art review*, Advances in Structural Engineering, (2018) Vol.21, No.10, pp.1562-1584.

[10] A. Carrella, D.J. Ewins, *Identifying and quantifying structural nonlinearities in engineering applications from measured frequency response functions,* Mechanical Systems and Signal Processing, Vol. 25, No. 3, (2011), pp. 1011-1027.

[11] K. Yasuda, S. Kawamura, K. Watanabe, *Identification of Nonlinear Multi-Degree-of-Freedom Systems : Identification Under Noisy Measurements,* JSME international journal, Ser. 3, Vibration, control engineering, engineering for industry, Vol. 31, No. 3, (1988), pp. 502-509.

[12] E.F. Crawley, A.C. Aubert, *Identification of nonlinear structural elements by force-state mapping,* AIAA Journal, Vol. 24, No. 1, (1986), pp. 155-162.

[13] E.F. Crawley, K.J. O'Donnell, *Force-state mapping identification of nonlinear joints,* AIAA Journal, Vol. 25, No. 7, (1987), pp. 1003-1010.

[14] G. Kerschen, J.C. Golinval, K. Worden, *Theoretical and experimental identifcation of a nonlinear beam,* Journal of Sound and Vibration, Vol. 244, No. 4, (2001), pp. 597-613.

[15] M. Feldman, *Nonparametric identification of asymmetric nonlinear vibration systems with the Hilbert transform,* Journal of Sound and Vibration, Vol. 331, No. 14, (2012), pp. 3386-3396.

[16] M. Feldman, *Hilbert transform methods for nonparametric identification of nonlinear time varying vibration systems,* Mechanical Systems and Signal Processing, Vol. 47, No. 1, (2014), pp. 66-77.

[17] K. Worden, J.J. Hensman, *Parameter estimation and model selection for a class of hysteretic systems using Bayesian inference,* Mechanical Systems and Signal Processing, Vol. 32, (2012), pp. 153-169.

[18] P.L. Green, *Bayesian system identification of a nonlinear dynamical system using a novel variant of Simulated Annealing,* Mechanical Systems and Signal Processing, Vol. 52-53, (2015), pp. 133-146.

[19] A. Ben Abdessalem, N. Dervilis, D. Wagg, K. Worden, *Model selection and parameter estimation in structural dynamics using approximate Bayesian computation,* Mechanical Systems and Signal Processing, Vol. 99, (2018), pp. 306-325.

[20] J. Prawin, A.R.M. Rao, *Nonlinear identification of MDOF systems using Volterra series approximation.* Mechanical Systems and Signal Processing, Vol. 84, (2017), pp. 58-77.

[21] M. Haroon, D.E. Adams, Y.W. Luk, A.A. Ferri, *A time and frequency domain approach for identifying nonlinear mechanical system models in the absence of an input measurement,* Journal of Sound and Vibration, Vol 283, No. 3, (2005), pp. 1137-1155.
[22] J. Taghipour, H.H. Khodaparast, M.I. Friswell, H. Jalali, *An Optimization-Based Framework for Nonlinear Model Selection and Identification*, Vibration 2 (4), 311-331.
[23] X. Wang, G.T. Zheng, *Equivalent Dynamic Stiffness Mapping technique for identifying nonlinear structural elements from frequency response functions,* Mechanical Systems and Signal Processing, Vol. 68-69, (2016), pp. 394-415.
[24] J. Taghipour, M. Dardel, *Steady state dynamics and robustness of a harmonically excited essentially nonlinear oscillator coupled with a two-DOF nonlinear energy sink*, Mechanical Systems and Signal Processing, Vol. 62-63, (2015), pp. 164-182.
[25] J. Taghipour, M. Dardel, M.H. Pashaei, *Vibration mitigation of a nonlinear rotor system with linear and nonlinear vibration absorbers*, Mechanism and Machine Theory, 2018 (128), 586-615.
[26] J. N. Reddy, An Introduction to the Finite Element Method, McGraw-Hill, New York, 2005.